An Acad Bras Cienc (2022) 94(Suppl.1): e20210114 DOI 10.1590/0001-3765202220210114
Anais da Academia Brasileira de Ciências | *Annals of the Brazilian Academy of Sciences*
Printed ISSN 0001-3765 I Online ISSN 1678-2690
www.scielo.br/aabc | www.fb.com/aabcjournal

GEOSCIENCES

Sedimentary evidence of glacial entrainment at Patriot Hills and Union Glacier moraines, Ellsworth Mountains, West Antarctica

VANESSA COSTA, KÁTIA K. ROSA, ALLAN SANDES, CAROLINE DELPUPO & ROSEMARY VIEIRA

Abstract: This work aims to analyze and compare the sedimentological data of Ellsworth Mountains, West Antarctica: Patriot/Independence Hills and Union Glacier, and how sedimentological data can be used to infer sediment entrainment. Particular attention was concentrated on morainic deposits. Remote sensing data was used in the identification of deposits and the ice flow; granulometric, morphoscopic, and geochemical analyses were applied to investigate the sedimentary origin and transport history. Sediment rich in Si Al, Fe, and Ca predominate in Independence Hills and Rossman Cove but Ca prevails in Elephant Head. CIA indicated low values, which depict low chemical weathering processes. X-ray diffraction reveals the presence of minerals that constitute the local rocks in the Union Glacier area, and from the unexposed basement rocks in Independence Hills. Principal Component Analysis and Cluster Analysis results suggest the sediment is related to the local rocks in the Union Glacier and distinct exotic sources in Independence Hills, associated with far-traveled sediment. It is also observed the influence of distinct processes of entrainment sediment on its granulometric and morphoscopic characteristics.

Key words: Antarctica, Ellsworth Mountains, sedimentology, geochemistry, glacial geomorphology.

INTRODUCTION

Past fluctuations of the West Antarctic Ice Sheet (WAIS) are of fundamental concern for the possibility of the Antarctic ice sheet collapse in the future and a consequent rise in global sea level (Mercer 1978, Chen et al. 2006, Hein et al. 2016a, Turney et al. 2019, Naughten et al. 2021). The WAIS volume has undergone fluctuations since the Quaternary period, from ice expansion events, covering local mountains and valleys, to the retraction events with exposure of subglacial topography. The Antarctic ice sheet has diminished in size since the Last Glacial Maximum (LGM) in all sectors (Fogwill et al. 2012, Joughin et al. 2014, Rignot et al. 2014), and ice loss will likely continue over the coming decades and centuries (Pattyn & Morlighem 2020).

This reduction in size and thickness has generated ice-free areas. They manifest in many forms, including exposed mountain tops (nunataks), cliffs, scree slopes, ice-free valleys, coastal oases, and islands, ranging in size from less than 1 km^2 to thousands of km^2, and can be separated by meters to hundreds of kilometers (Lee et al. 2017). There are few ice-free areas in the interior of Antarctica that could preserve geomorphologic and sedimentological evidence for the ice elevation changes. Thus, as more glacial sediment data become available,

a greater understanding of bedrock geology, geomorphic processes, as well as glaciological processes follow (Licht & Hemming 2017).

Important features for understanding the history of the ice sheet are the several types of moraines formed in the ice-free areas. Blue-ice areas (BIAs) and associated deposits, located mostly in mountainous regions of Antarctica, are sites that have the potential to preserve long-term records of ice sheet changes (Kassab et al. 2019).

Blue-ice areas are a rare feature estimated to cover 120,000 km^2 and occupy between 0.8 and 1.6% of the continent (Winther et al. 2001). There are two main types of blue-ice area: (a) interior zones associated with steepening and convergent ice-surface slopes that cause the katabatic winds to accelerate and, (b) those associated with mountains and nunataks (Sugden & Hall 2020).

The blue-ice area is found where the ablation is triggered by the katabatic winds from the polar plateau that remove the snow from the ice surface and by sublimation (Birtanja 1999, Sinisalo & Moore 2010). The older ice may rise to the surface by the buttressing effect due to submerged or emerged bedrock obstacles (Corti et al. 2008), and moraines can be formed in certain blue-ice areas where the topography concentrates airflow in depressions or the vicinity of nunataks (Fogwill et al. 2012). These glacial and atmospheric processes cause previously horizontal englacial layers to flow up toward the mountain front (Winter et al. 2016), exposing glacially entrained sediment clasts that often exhibit glacial abrasion, in the form of subangular to subrounded shapes and millimeter-scale striations (Turney et al. 2013).

The moraines formed in these areas are known as blue-ice moraines (Fogwill et al. 2012, Hein et al. 2016a, Sugden et al. 2017). With the development of provenance techniques, such as geochemical and cosmogenic isotope analysis, and geomorphic observations, attention has more recently focused on the moraines and surface debris in various blue-ice areas, the implications for ice flow, the history and the dynamic of the ice sheet (Bader et al. 2017, Akçar et al. 2020).

In the Weddell embayment, the Ellsworth Mountains (79° 46'S, 83° 24'W) serve as one of these significant ice-free areas, corresponding to 4.2% of the total blue-ice area cover of Antarctica - 120,000 km^2 (Winther et al. 2001, Sinisalo & Moore 2010, Delpupo et al. 2017). The blue-ice area formed on the leeward side of Patriot Hills (80°18'S, 81°22'W), southern Ellsworth Mountains has an area of approximately 12,62 km^2, with no significant changes in areal extent (Wendt et al. 2009, Rivera et al. 2014a, Turner et al. 2019). The blue-ice area at Union glacier (79°46'S, 83°24'W) is located at the narrowest section of the glacier (7 km wide), where the Union and Schanz glaciers merge (Rivera et al. 2010, 2014a).

Previous works presented the age of the moraines and till in Patriot, Independence, and Marble Hills using cosmogenic ^{10}Be, ^{26}Al, ^{36}Cl, and ^{21}Ne analyses (Fogwill et al. 2012, Hein et al. 2016a, b), addressing questions concerning ice sheet (in)stability. Winter et al. (2019) used ice-penetrating radar to examine englacial sediments in Patriot and Independence Hills blue-ice areas. Costa et al. (2017) investigate the geomorphological and sedimentological aspects of Union Glacier. Nevertheless, a lack of data still limits the knowledge of sediment provenance, transport, and deposition processes in this part of the Ellsworth Mountains. The purpose of this article is to analyze the sedimentary processes on the formation of moraines in blue-ice areas of the southern part of Ellsworth Mountains: Patriot / Independence Hills and Union Glacier, based upon the granulometric, clast shape, geochemical, and mineralogical composition

analysis of the sediment, and to infer the provenance and the processes on sediment transported and deposited by the glaciers in these areas.

REGIONAL SETTING

Ellsworth Mountains (Figure 1a) are within 50 km of the grounding line, which marks the interface between the grounded ice sheet and the floating Filchner-Ronne Ice Shelf in Hercules Inlet, a sensitive location to changes in ice thickness in the Weddell Sea (Hein et al. 2016b). Numerous valleys characterize the Ellsworth Mountains; they were formed by glacial erosion and have a high concentration of surface deposits and erosional features that contain records of the geological, climatic and, environmental history. The mountains form an NNE-SSW trending range approximately 445 km in length, centered about 79°S 84°W, and are divided into two geographically distinct ranges: Sentinel Range to the north and Heritage Range to the south (Denton et al. 1992). Meteorological data collected at Union Glacier presented an average temperature, in the period 2008-2013, -20.6º C, an absolute minimum temperature of -42.7º C in August 2008, and an absolute maximum of 0.5º C recorded in January 2010 (Rivera et al. 2014b). In a more recent study in the same area, the mean daily air temperature, in the period 2010-2018, was -21.3±8.5 °C with an absolute minimum of -46.8 °C recorded in July 2017, and an absolute maximum of 3.3 °C measured in

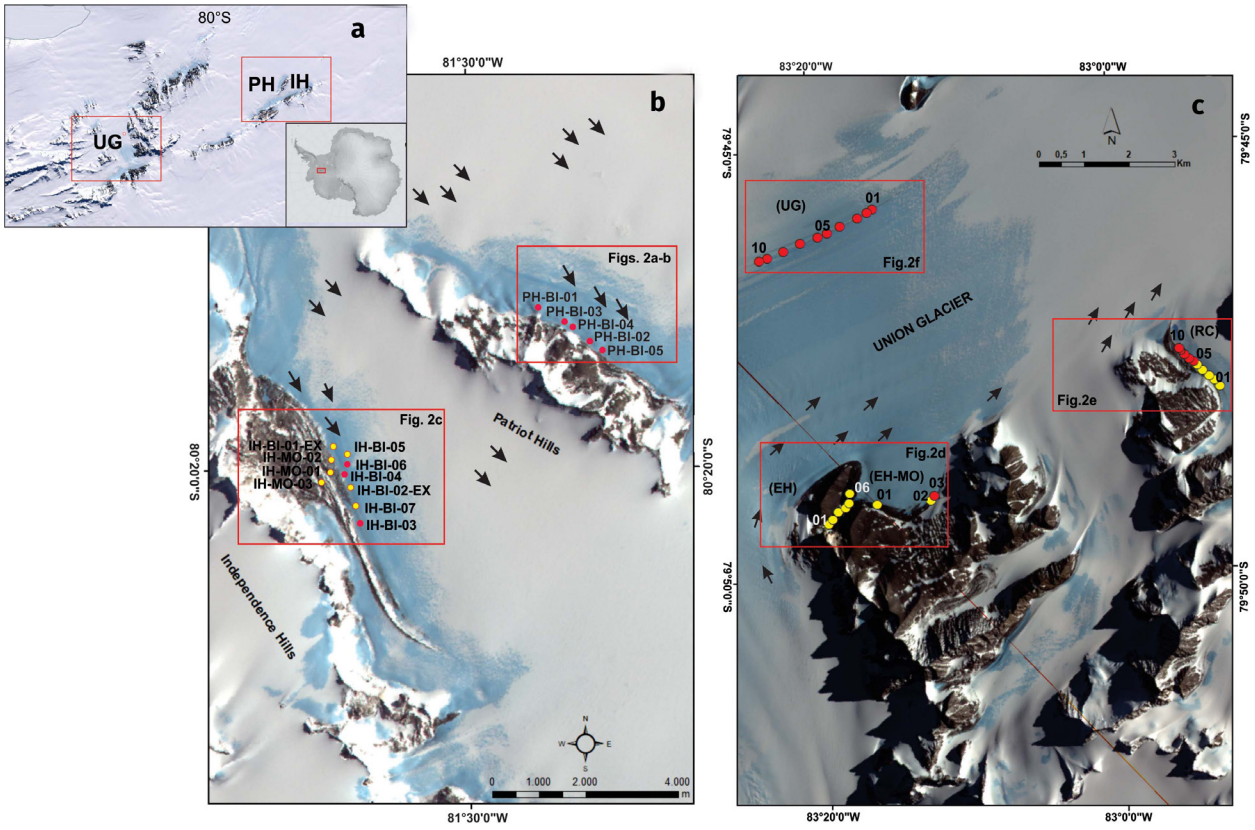

Figure 1. Location of sampling sites in the Independence - IH / Patriot Hills - PH (1a-b) and in Union Glacier area – UG (1a-c), Ellsworth Mountains, and their corresponding indication in Figure 2. (red boxes). Adapted from Antarctic Digital Database and ASTER imagery (2007/2010). Yellow dots indicate samples with fine fractions (<0.062mm). The arrows indicate glacier flow (based on Turney et al. 2013, Rivera et al. 2010, Gomez et al. 2019).

February 2013 (Hoffmann et al. 2020). In these regions, strong katabatic winds (± 30 ms-¹ - Hoffmann et al. 2020) and low accumulation predominate (~ 50 kg m² / a-¹ - Casassa et al. 2000). The precipitation is principally delivered via frontal systems originating in the Weddell Sea (Wendt et al. 2009).

The Patriot Hills and Independence Hills compose the southernmost peaks of the Heritage Range and comprise several deglaciated and ice-filled valleys (Fig. 1a) (Vieira & Simões 2011, Vieira et al. 2012). They comprise one of many Antarctic nunataks, which act as obstacles to katabatic winds (Rivera et al. 2014a). Parallel to these mountains the Horseshoe Glacier flows northwest-southeast at 8-12 m/a (Casassa et al. 2004, Rignot et al. 2017) through Horseshoe Valley with an approximate length of 60 km, extends 1300m below present sea level, and channelizes ice toward the Filchner-Ronne Ice Shelf, at Hercules Inlet (Casassa et al. 2004, Sugden et al. 2017, Winter et al. 2019). Horseshoe Valley is separated from northward-flowing Union Glacier by Enterprise Hills (Webers et al. 1992). Ice-thickness values of about 1300 m exist toward the center of Horseshoe Valley, and a maximum ice thickness of 383 m was measured near the center of the blue ice field of Patriot Hills (Casassa et al. 1998).

Patriot, Independence, and Marble Hills rocks comprise three major units of Minaret Formation limestones of the Heritage Group (Supplementary Material - Figure S1): (1) conglomerate with limestone boulders; (2) well-bedded dark-gray limestone; and (3) white limestone/marble beds (Spörli et al. 1992, Webers et al. 1992, Curtis & Lomas 1999). Thicker carbonate succession is present in Independence Hills (Curtis & Lomas 1999). Horseshoe Valley is surrounded to the northeast by rocks from Crashite Quartzite Group, in Enterprise Hills, which is composed mainly by quartzite followed by sandstones, and from Minaret Formation in Liberty Hills, Marble Hills, and Patriot Hills, to the southwest (Spörli 1992, Webers et al. 1992).

The identification of weathered and iron-stained erratics, yielding a cluster of exposure ages >400 cal ka (Fogwill et al. 2012), on the uppermost weathered slopes of the Patriot Hills implies that there has been no inundation by the WAIS over the surrounding escarpments during the last glacial cycle and that Horseshoe Valley has remained glaciologically isolated (Turney et al. 2013).

Union Glacier (79°45"S / 82°30'W), 70 km north from Patriot Hills, approximately, has a total area of 2561 km^2 and length of 86 km, from the ice divide with the Institute Ice Stream down to the grounding line of Constellation Inlet on the Ronne Ice Shelf (Rivera et al. 2014a). The glacier is fed by several tributary glaciers flowing from the interior cirques and accumulation basins between mountain ridges (Denton et al. 1992). The maximum ice thickness at this region is 1540 m, with a maximum snow ice boundary layer at 120 m (Rivera et al. 2014b).

The area comprises Cambrian rocks of the Union Glacier Formation, which is overlain by Hyde Glacier Formation and Drake Icefall Formation from the Heritage Group (Spörli 1992 – Figure S1). The dominant rock types in the Union Glacier Formation are dark green tuffaceous diamictite, calcareous sandstone, calcareous conglomerate, and quartzite, with high proportions of mica, quartz, and chlorite. The Hyde Glacier Formation includes a wide variety of volcanogenic sedimentary rock types: argillite, quartzite, phyllite, and conglomerates, with clasts of rock fragment, quartz, plagioclase, mica, calcite, and dolomite (Webers et al. 1992). Reworked carbonate clasts are found in the Middle Cambrian Union Glacier, the Conglomerate Ridge Formations, and the Permo-Carboniferous Whiteout Conglomerate (Spörli et

al. 1992). Autochthonous carbonates are found in the Middle Cambrian Drake Icefall Formation and the Minaret Formation (Buggish & Webers 1992).

Elephant Head valley is approximately 1000 m long; the upper and wider sector is 900 m high and > 200 m above the blue-ice area, while the confluence zone with the Union Glacier corresponds to the narrowest sector, which is blocked by the moraine developed on the Union glacier blue-ice area. The valley is bordered from one side by a mountain crest with summits up to 1000 m that rise between 100 – 300 m above the present blue-ice area, including the Rhodes Bluff massif, a white, massive marble-like limestone (Spörli & Craddock 1992); on the other side quartzite crest (Bockheim & Schaefer 2015). The slopes are mantled by locally derived and weathered clasts that also cover partially the moraines. Discontinuous sandstone blocks cover the ground of the valley, between low rounded dome-like bodies of conglomerates and carbonate. The conglomerate blocks consist largely of medium to large pebbles, with some incrusted ripple marks (Costa et al. 2017).

Figure 2. Photographs showing: blue-ice moraines in Patriot Hills (2a-b), in Independence Hills (2c), and Union Glacier (2d); ice-cored moraines in Rossman Cove (2e); medial moraine in Union glacier (2f); recessional moraines in Elephant Head valley (2g-h). The location of sampling sites is indicated in Figure 1 (red boxes).

MATERIALS AND METHODS

Fieldworks and sampling

Fieldworks were conducted during December / January 2008/09 in Patriot and Independence Hills (Figure 1b), and during December / January 2011/12 in the Union Glacier area (Figure 1c). The glacier marginal landforms and depositional features were identified in ASTER visible\near-infrared (VNIR) color composite scenes (RGB 321), and verified during field activities with a portable GPS, with an error of about 3 m (Figures 1 and 2). In Patriot and Independence Hills, the sediment was sampled in the blue-ice moraines (Figure 2 and Table I). In the Union Glacier area the sediment was sampled in the moraine at the Union Glacier margin toward Mount Dolence, Rossman Cove moraine, and in Elephant Head valley moraines. Except for Elephant Head valley, all sampled moraines have developed on the blue-ice areas, and massive ice was recorded below the debris cover.

The sediment from moraines was collected in shallow cavities in the debris cover and blue-ice surface, stored in airtight coded plastic bags, uniquely identifying each sample, and frozen until laboratory analysis. Control points (GPS coordinates and altitude), photographs, and observations of the surrounding environment

Table I. Localization of the sampling sites in Patriot Hills, Independence Hills, and Union Glacier area.

Area	Sample ID*	Latitude	Longitude
	PH-BI-01	80°19'11.7''S	81°25'20.5''W
	PH-BI-02	80°19'11.7''S	81°25'20.5"W
Patriot Hills	PH-BI-03	80°19'18.6''S	81°23'48.2''W
	PH-BI-04	80°19'18.9''S	81°23'44.7''W
	PH-BI-05	80°18'49''S	81°31'18.8''W
	IH-BI-01-EX	80°20'56.8''S	81°39'02.3''W
	IH-BI-02_EX	80°21'03.2''S	81°38'38.4''W
	IH-BI-03	80°21'34.07''S	81°36'50.6' W
	IH-BI-04	80°20'58.6''S	81°38'55.2'W
Independence Hills	IH-BI-05	80°20'58.6''S	81°38'57º W
	IH-BI-06	80°20'57.7''S	81°39'01.6"W
	IH-BI-07	80° 21'12.9''S	81°38'05.8"W
	IH-MO-01	80° 20'59.7''S	81°39'19.3"W
	IH-MO-02	80° 21'15.2''S	81°38'24.7''W
	IH-MO-03	80° 21'5.2''S	81°39'22.1"W
	UG-01	79°45'51.8"S	83°14'55.0''W
	UG-02	79°45'59.1''S	83°15'09.2''W
	UG-03	79°45'66.6''S	83°15'89.5''W
	UG-04	79°45'73.7'S	83 16'68.0''W
Union Glacier	UG-05	79°45'81.0''S	83°17'58.5''W
	UG-06	79°45'86.1''S	83°18'22.0''W
	UG-07	79°45'86.1''S	83°18'98.9''W
	UG-08	79°45'91.7''S	83°19'81.8''W
	UG-09	79°45'97.5''S	83°20'72.8''W
	UG-10	79°46'03.5''S	83°21'57.2''W
	RC -01	79°47'89.2''S	82°53'36.9''W
	RC -02	79°47'84.9''S	82°53'53.6''W
Rossman Cove	RC -03	79°47'80.8''S	82°53'74.7''W
	RC -04	79°47'75.7''S	82°54'01.1''W
	RC -05	79°47'71.7''S	82°54'29.2''W
	RC-06	79°47'60.9"S	82°54'58.4''W
	RC-07	79°47'60.9"S	82°54'85.0''W
	RC-08	79°47'56.2S	82°55'09.6''W
Rossman Cove	RC-09	79° 47' 50.3'S	82°55 39.7''W
	RC-10	79°47'43.9'S	82°55'71.1''W
	EH-01	79°49'11.1''S	83°16'10.7''W

Table I. Continuation.

	EH-02	79°49'29.8''S	83°20'42.6''W
Elephant Head Valley	EH-03	79°49'23.8''S	83°18'92.8''W
	EH-04	79°49'13.1''S	83°18'42.5''W
	EH-05	79°49'28.9''S	83°20'02.0''W
	EH-06	79°49'22.9''S	83°19'07.7''W
	EH-MO-01	79°48'70.9''S	83°05'20.7''W
Elephant Head Moraine	EH-MO-02	79°48'70.8''S	83°05'19,8''W
	EH-MO-03	79° 48' 70.6''S	83° 05' 19,5''W

***PH- Patriot Hill; IH- Independence Hills; UG – Union Glacier; EH - Elephant Head; RC – Rossman Cove; BI – Blue Ice; EX- External; MO – Moraine.**

were recorded. All samples were kept in a snow trench (1.5 m deep) during the expedition period, in a freezer during the return trip, and in the laboratory until analysis. Clasts with a major axis >16 mm (pebble fraction) were collected for the description of clast form. Before laboratory analysis, all samples were freeze-dried for 3 days, subsequently dry-sieved at range 8 mm a 0,062 mm, and gently disaggregated.

Granulometric and shape analysis

The particle size distribution of sand fractions was obtained by the CAMSIZE analyzer, and the silt samples were analyzed by the Malvern laser light scattering granulometer. These analyses were performed in the Sedimentology Laboratory, Institute of Geosciences, Fluminense Federal University (UFF). The software Gradistat (Blott & Pye 2001, 2007) calculated the statistical analysis. The weight of the granulometric fractions was calculated as weight percentages with a digital scale (instrument error of 0.001 g).

Clast analysis was carried out with the aid of a binocular microscope to identify the clast surface features, such as striation. Clast size and shape measurement was carried out on 100 clasts with a major axis >16 mm in the digital caliper to visually determine the relative size of the three orthogonal axes: *a* (longest), *b* (intermediate), and *c* (shortest) (Evans & Benn 2004, Hubbard & Glasser 2005). The index denominated C_{40}, the ratio between the axes c / a ≤ 0.4, discriminates clasts with platy features and clasts with cubic features, to determine those that have been rounded through subglacial work (Evans & Benn 2004).

Roundness (gravel size / 4-16 mm) was obtained with the aid of a binocular microscope using a visual comparison chart or descriptive criteria provided by Benn & Ballantyne (1994). The estimated roundness classes for each sample were translated into percentages and plotted as frequency distributions. The percentages of very angular (VA) and angular (A) were added to calculate the RA-index. RWR-index (% of rounded and well-rounded clasts) was also conducted according to the method proposed by Benn & Balllantyne (1994), and by Evans & Benn (2004), to distinguish between erosional, transportational, and depositional clast histories (Lukas et al. 2013). The graphs of granulometric and shape analysis were performed with GraphPad Prism software.

Lithological and geochemical analysis

For the lithological analysis, the adopted sample size was clasts > 2 mm, gravel fractions (n = 200). Clasts were examined using a binocular microscope, subdivided into classes based upon their lithological properties, and compared to

the available mineral database on the web (www.webmineral.com), and in the literature, such as the works of Klein & Dutrow (2012) and Perkins (2014).

The major chemical elements of 20 sediment samples (Supplementary Material - Table SII) were defined by the fine-grained fractions (<0.062mm) in Energy Dispersive X-ray Fluorescence (ED-XRF) Spectrometer (SHIMADZU EDX-720). Some of the samples could not be analyzed because there was no fine-grained sufficient amount. The sediment was prepared in the Sedimentology Laboratory of the Institute of Geosciences at Fluminense Federal University and analyzed in the Laboratory of Reactors, Kinetics, and Catalysis in the Chemical Engineering Department at Fluminense Federal University.

The X-ray fluorescence spectrometry does not destroy the sample, so it was possible to use the same aliquot for the mineralogical analysis. The crystalline XRD method facilitates the identification of the main minerals of the sediment (Chipera & Bish 2013). The mineralogical composition was determined to ascribe provenance, by X-ray diffraction by a Brucker D8 Advance x-ray diffractometer (XRD) in the X-Ray Diffraction Laboratory, Physics Institute at Fluminense Federal University. Each sample was scanned from 2° 2θ to 70° 2θ with CuKα radiation (40 kV and 40 mA), using a 0.02° 2θ scanning step and 0.5 s counting time per step, with an LYNXEYE detector. Minerals were identified from their characteristics peaks with DIFRA EVA software, using USGS (United States Geological Survey) mineral database.

One approach to estimate the degree of chemical weathering by Chemical Index of Alteration – CIA (Nesbitt & Young 1982) was calculated. Usually, the CIA ranges between 50 for fresh rocks and 100 for highly residual clay. CIA values were calculated according to the formula (Nesbitt & Young 1982).

$$CIA = [Al_2O_3 / (Al_2O_3 + K_2O + Na_2O + CaO)] \times 100 \quad (1)$$

Cluster Analysis (CA) and Principal Component Analysis (PCA) were applied to obtain similarities and differences between the sampling sites and correlations between chemical elements. Logarithmic transformation was used before the application of multivariate statistics. The cluster analysis is used in this work as an exploratory tool, not as a statistical test. The dendrograms were elaborated from the Paired, Simple, and Ward methods to detect similarities and differences between sample sites in the Patriot / Independence Hills and Union glacier areas and correlations between variables. Euclidean distance was used for the distance measured. For the Principal Component Analysis, the correlation coefficient was used as the initial matrix of similarities, to eliminate the effect of scale (Alfonso et al. 2015). Multivariate analysis was carried out in Paleontological Statistics (PAST) 4.01 software.

RESULTS

Glacial geomorphology

Glacial and periglacial landforms could be identified based on visual interpretation of ASTER imagery and fieldwork observations. Three main types of moraines were distinguished: blue-ice moraines (Figs. 2a-e), medial moraine (Fig. 2f), and moraines of recession along the ice-free valleys (Figs. 2g-h).

There are marked differences between the Patriot and Independence Hills and the Union Glacier area concerning the depositional features. In the leeward side of Patriot Hills and Independence Hills prominent well-defined parallel ridges of blue-ice moraines up to 10m high extend for more than 5 km (Figs. 2a-c).

Patriot and Independence Hills moraines have irregular topography (Fig. 2b) and several melt ponds. In Independence Hills, the blue-ice moraines have distinct colored bands. In the blue-ice area, far from the mountain slopes, both in Patriot Hills and Independence Hills, straight sediment ridges extend in the sub-ice surface that correspond to the englacial debris band emerging to the ice surface. (Figs. 2a-c).

In contrast, Mount Dolence and Elephant Head create an embayment along the lateral margin of the Union Glacier (Fig. 1). The morphology of the moraine is curved following the shape of the embayment, and the surface is characterized by relatively irregular topography, but with no parallel ridges (Fig. 2d). Large boulders are found on the surface. On the other hand, morainic ridges are observed at Rossman Cove (Fig. 2e). The entire moraine is ice-cored, but without large boulders on the surface. A long moraine belt extends approximately 2.35 kilometers in the central part of Union Glacier, but no more than 1 meter high. (Fig. 2f). In Elephant Head valley five morainal ridges could be identified, but part of these deposits is covered by material from the lateral slopes.

Particle size and shape

Particle size analysis of samples of Independence and Patriot Hills blue-ice moraines shows the predominance of gravel, sandy gravel, and sand (Figure 3 and Table SI). Five sites presented a high proportion of gravel content (>87%): PH-BI-03, PH-BI-04, IH-BI-04, IH-MO-01, and IH-MO-02; and coarse sand fractions predominate in four samples: PH-BI-01, PH-BI-02, IH-BI-05, and IH-BI-06. In Independence Hills, silt content reaches 19.2 and 29.2% in the two sampling sites on the blue-ice area: IH-BI-02-EX and IH-BI-06. The region is subject to the strong katabatic winds favoring the concentration of gravels on the blue-ice surface.

In the three sampled areas in Union Glacier gravel and sandy gravel predominate at all

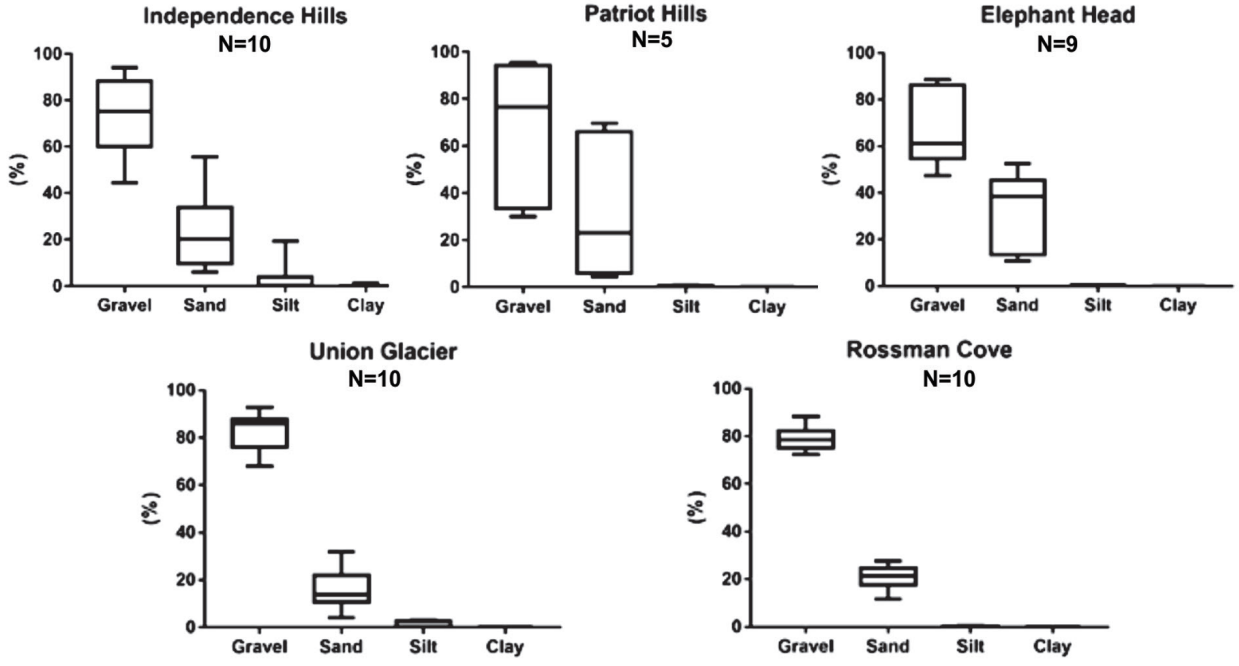

Figure 3. Box plots of particle size data (Table SI). The box outlines the middle 50% of data (2nd and 3rd quartiles). The line inside the box represents the median value of the whole data set, and the whiskers show the greatest/least values.

sampling sites. In the Union glacier central moraine, sediment comprises over 68% of gravel content. Sand content varies between 4-24% in all sampling sites. The content of silt does not exceed 3%. The samples collected on ice-cored moraines in Rossman Cove comprise 72-88% gravel and 11-27% sand content. The content of fine material does not exceed 0.4%. The morainic sediment along the Elephant Head valley shows the predominance of gravel (47-70%) and sand (29-52%); silt content does not exceed 0.5%. The valley is partially protected and sandy fraction is recorded in samples.

The particle shape is dominated by angular (A) and subangular (SA) grains in Patriot and Independence Hills sediment, whilst subrounded grains predominate in Rossman Cove, Elephant Head and Union Glacier moraines sediment, followed by subangular clasts. Very angular and well-rounded materials are absent (Figure 4, Table SI). A high C_{40} index in all sampling sites (Figure 4, Table SI) indicates unmodified

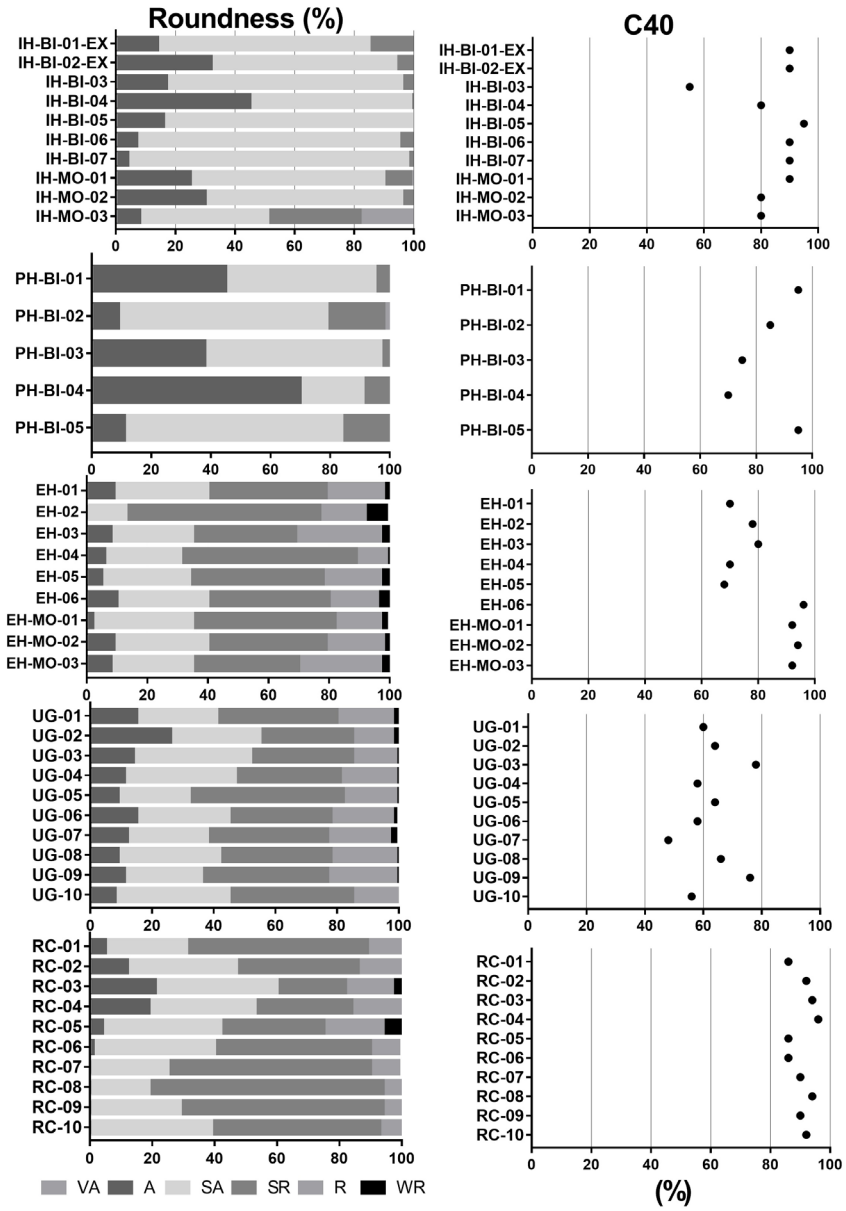

Figure 4. Shape characteristics of clasts from moraine deposits, subdivided by roundness category (left panel): Very Angular (VA); Angular (A); Sub Angular (SA); Sub Rounded (SR); Rounded (R); Well Rounded (WR), and C40 values (right panel). Independence Hills (IH); Patriot Hills (PH); Elephant Head Valley (EH); Elephant Head Moraine (EH-MO); Union Glacier (UG); Rossman Cove (RC).

frost-weathered debris. Co-variance plots using both RA-C_{40} and RWR-C_{40}, which effectively differentiate passively- and actively-transported clasts (Benn & Ballantyne 1994), are shown in Figure 5 and display high C_{40}, medium RA, and low RWR, which point to the processes of the entrance of clasts extraglacial/supraglacially, i.e., passively transported (Lukas et al. 2013). The RWR-C_{40} approach depicts more clearly the passively-transported clasts, but RA-C_{40} points to distinct sediment shape features and distinct transport processes (Fig. 5). In Figure 4 (right panel) Independence (IH) and Patriot Hills (PH) show clasts varying from moderate-high to high RA index (>50% and 70%, respectively). IH-BI-03 sampling site has clast with the lowest C_{40}. In Union Glacier (UG) the clasts also have a moderate-high C_{40} index. Elephant Head clasts vary in C_{40} values: they are lower in the interior of the valley and higher in the blue-ice area. In Rossman Cove, the clasts have a C_{40} index >80%.

Sediment composition and geochemical analysis

Lithological data (Fig. 6a-e) show the predominance of sandstone and quartzite in all samples of Patriot Hills, followed by other fragments (conglomerates, volcanic rocks, and quartz). In Independence Hills, sandstone also dominates in one of the samples (IH-BI-EX-02), but in the other sites, sandstone and quartzite are equally dominant. Quartzite predominates in all samples of Rossman Cove and Union Glacier. In Elephant Head valley carbonate, sandstone fragments, and quartzite are the main components of the gravel fractions (Fig. 6c). Carbonate and flat-lying sandstone from sand to boulder size range are scattered through the valley.

Fine-grained particles are present in the moraines but can be specially removed by the wind. Therefore, it was not possible to analyze these particles in all samples of morainic deposits, especially in Patriot Hills, Rossman Cove, and Union Glacier moraines, due to the insufficient amount of available fine-grained sediment.

X-ray fluorescence analysis of Independence Hills samples indicates a major concentration distributed amidst Si, Fe, Al, Ca, and K content (Fig. 7 and Table SII). Except for the IH-MO-03sample, which predominates Ca, the sediment in Independence Hills has a more balanced distribution of these elements. In the Union glacier area, Ca broadly predominates in

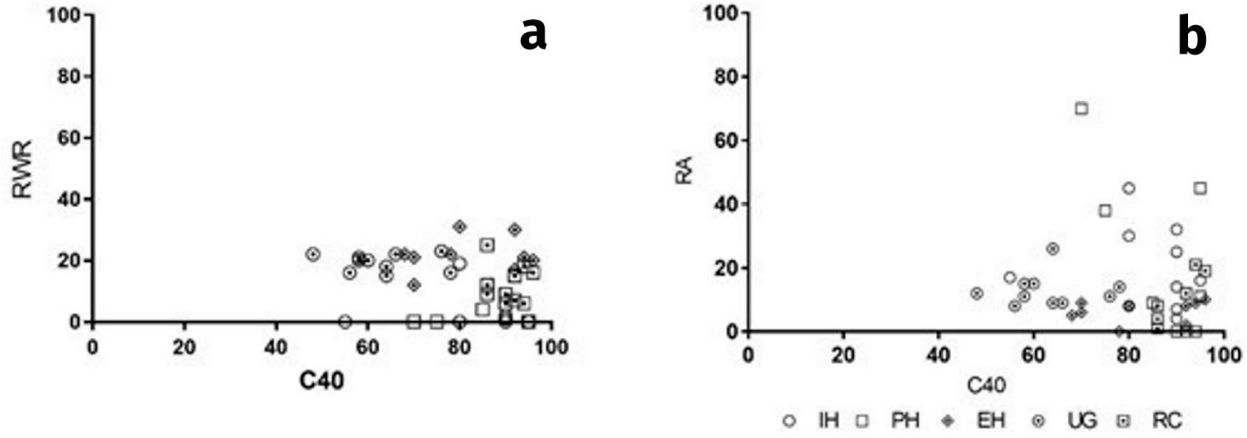

Figure 5. RA-C40 (5a) and RWR-C40 (5b) co-variance diagrams illustrating the different indices are used to discriminate between different samples.

Elephant Head valley, whereas in Rossman Cove Si is the major element, followed by Al, F, and Ca.

Chemical Alteration Index (CIA) points to no chemical weathering action in the sediment samples of both areas (Figure 7). The values above 85 indicate an intense chemical weathering and values between 45 and 55 indicate the absence or incipience of this process (Nesbitt & Young 1982). High values indicate intensive chemical weathering due to high precipitation and air temperatures, whereas low values may evidence a colder and/or more arid climate where physical weathering prevails. The CIA values in the Independence Hills vary between 2.0 and 45.2 (average – 29.3), and in Elephant Head valley vary between 0.7 and 7.1 (average – 2.2), and between 31.1 and 32.3 (average – 31.6) in Rossman Cove. The CIA values are variable in Independence Hills samples, in opposition to the regular values in Rossman Cove samples. In Elephant Head valley, the site with the highest Ca content, the CIA values are even lowest. Even though the low values were observed in Independence Hills a declining gradient in the transect blue-ice area/mountain walls was also apparent. The IH-MO-03 sample, closest to the mountain wall had the lowest CIA value (2.0). Therefore, the samples from the Union Glacier area (Elephant Head valley) and in Independence Hills (IH-MO-03 sample) that exhibit the lowest CIA values are the same that have predominant Ca content.

X-ray diffraction (XRD – Figures 8a-g) in Independence Hills reveals a prevalence

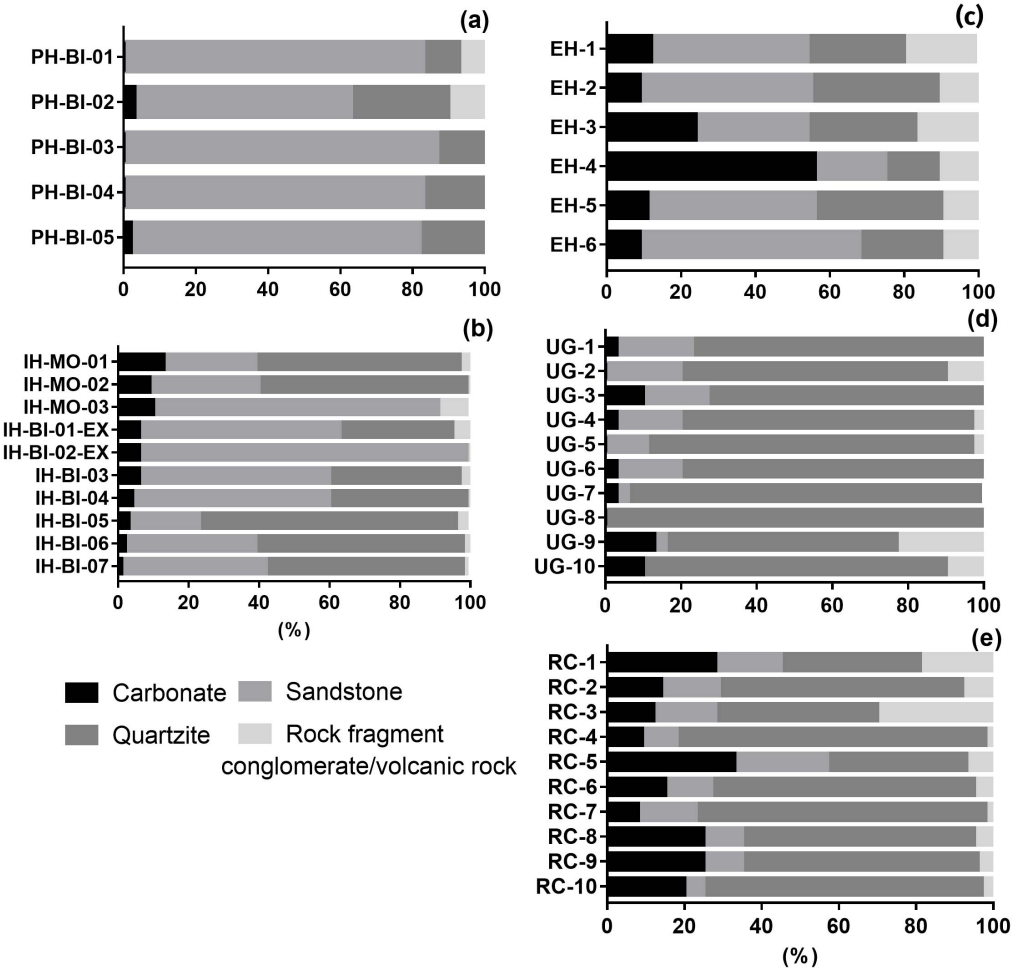

Figure 6. Percent lithology of the moraines by area and sample: Patriot and Independence Hills (6a, 6b); Union Glacier area (6c, 6d, and 6e).

of quartz in four of the six samples, followed by illite, muscovite, and kaolinite. Quartz is a principal product of many rocks making its origin uncertain. Albite predominates in the IH-BI-01 sample. Illite is a product of the physical weathering of micaceous minerals or hydrothermal alteration of muscovite. In sandstone, illite forms largely as a cement in primary pores (Milliken 2005).

In Elephant Head valley (Figs. 9a-f), calcite predominate; illite is absent in all samples, excepting the IH-MO-06 sample, located at the valley exit, in the blue-ice area. Quartz predominates in all Rossman Cove morainic samples (Figs. 10a-g) followed by illite and muscovite.

Statistical analysis

Cluster and Principal Component Analysis (PCA) were applied to obtain similarities and differences between sampling sites and correlations between chemical elements. Figures 11a-b show dendrograms for Independence Hills (A), and for Union Glacier area (Elephant Head and Rossman Cove) (B): Paired (1), Simple (2), and Ward methods (3), respectively. The Paired and Simple methods propose six groups: (1) IH-MO-3; (2) IH-MO-01; (3) IH-BI-05; (4) IH-BI-07 and IH_MO_02; (5) IH-BI-01-EX; (6) IH-BI-02-EX. The Ward method proposes five groups: (1) IH-BI-02-EX; (2) IH-BI-01-EX; (3) IH-MO-02 and IH-BI-07; (4) IH-BI-05 and IH-MO-01; (5) IH-MO-03. The group

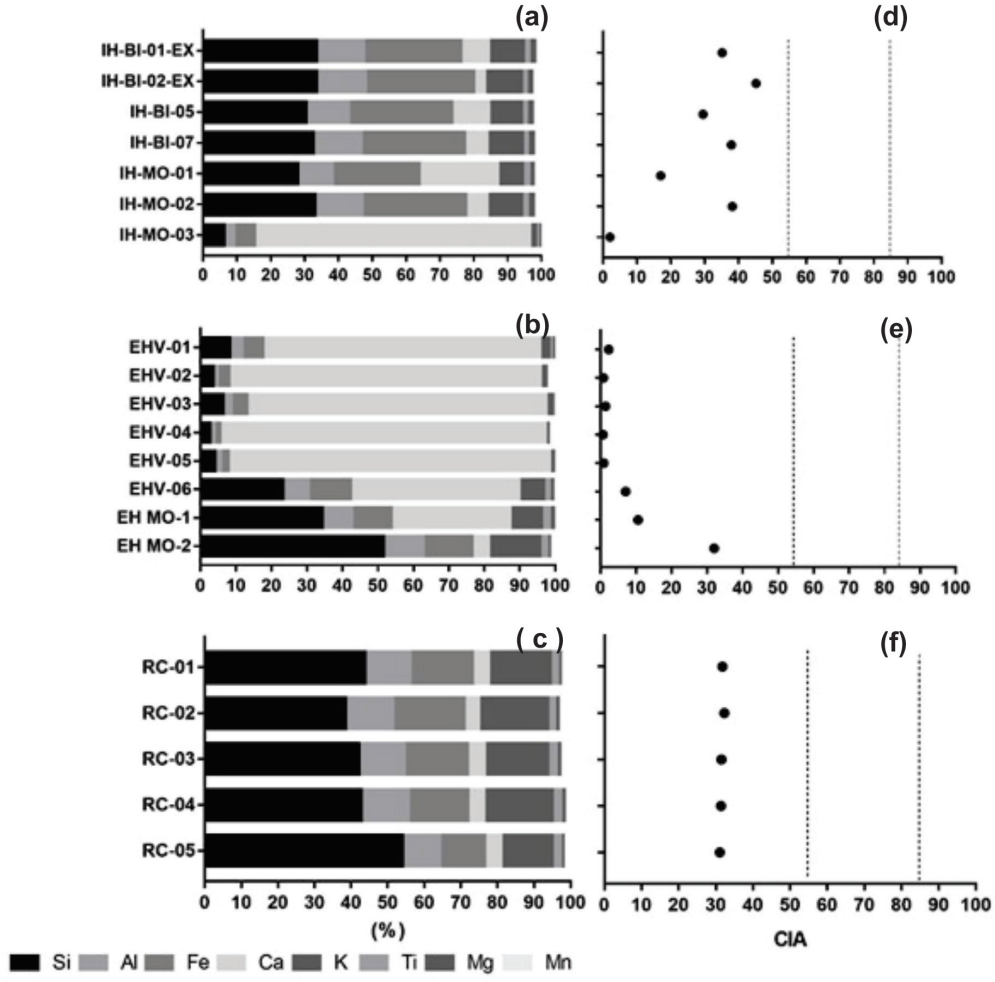

Figure 7. Histogram of elements concentration using XRF from the samples (7a, 7c, and 7e). Chemical Index of Alteration (7b, 7d, and 7f).

IH-MO-02 and IH-BI-07 are common in the three methods.

The results obtained by PCA for Independence Hills are shown in Figure 12a. Component 1 accounts for 95.4% of the variance and has high loadings of Al, K, Fe and Si, and negative loadings of Ca. The negative score (-6.2) is concentrated in the IH-MO-03 sample,

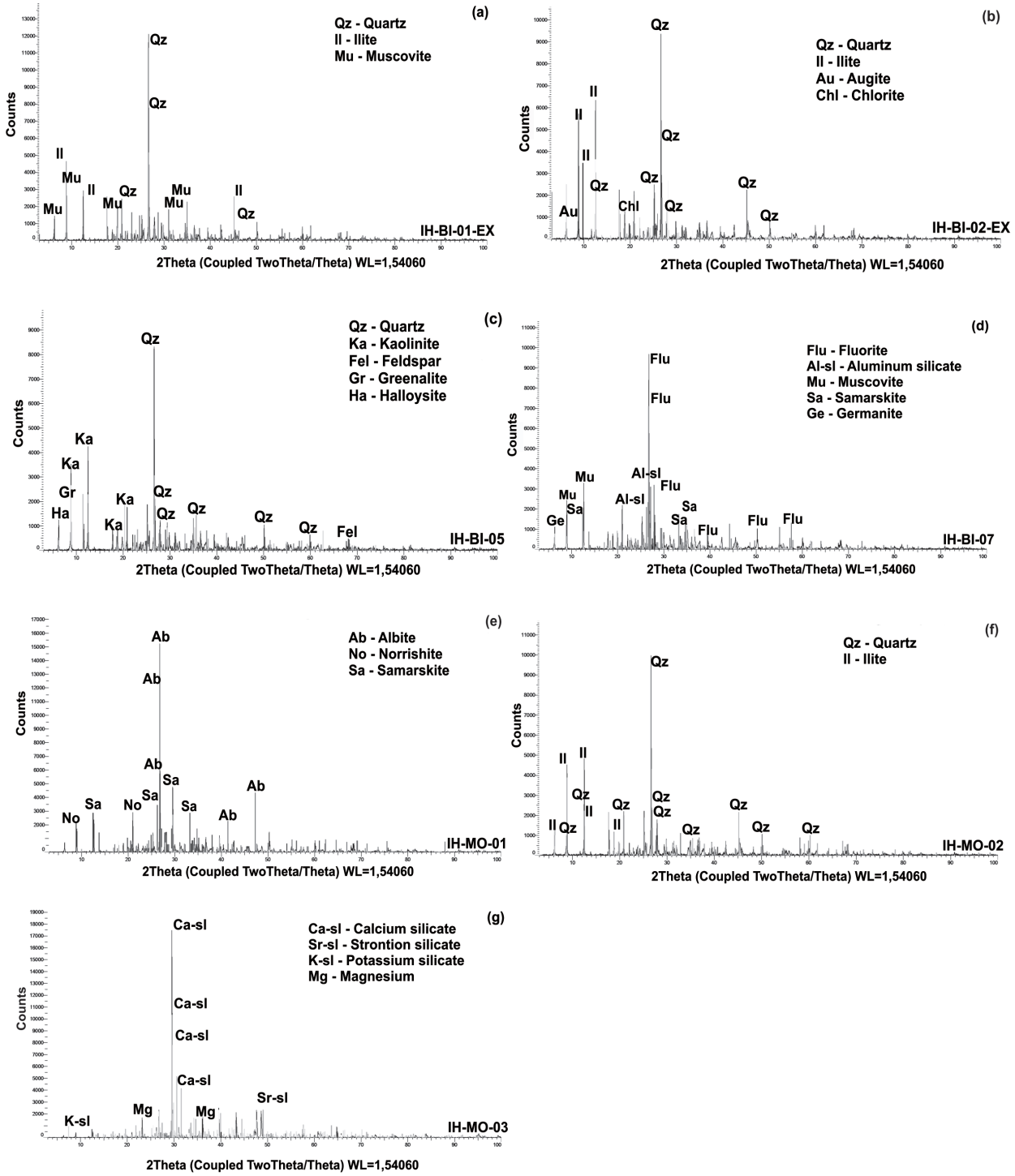

Figure 8. Diffratograms of fine-grained sediments of Independence Hills sampling sites.

the closest sampling site to the mountain wall. Component 2 explains 3.8% of the variance and has high loadings of Ca (0,8). The PC1 individualizes the IH-BI-03 sampling site, the closest site of the mountain wall.

In the Union Glacier area, the cluster analysis created eight groups by the Paired and Simple methods (Figure 11b): (1) EH_MO_2 and RC_05; (2) EH-01; (3) RC_03 and RC-04; (4) RC_02; (5) EH_06 and EH_MO_1; (6) EH_05; (7) EH_03 and EH_01; (8) EH_02 and EH_04. Eight groups were also formed following the Ward method: (1) EH_01 and EH_03; (2) EH_05; (3) EH_02 and EH_04; (4) EH_06 and EH_MO_1; (5) EH_MO_2 and RC_05; (6) RC_02; (7) RC_01; (8) RC_03 and RC_04. Some groups are present in the three methods:

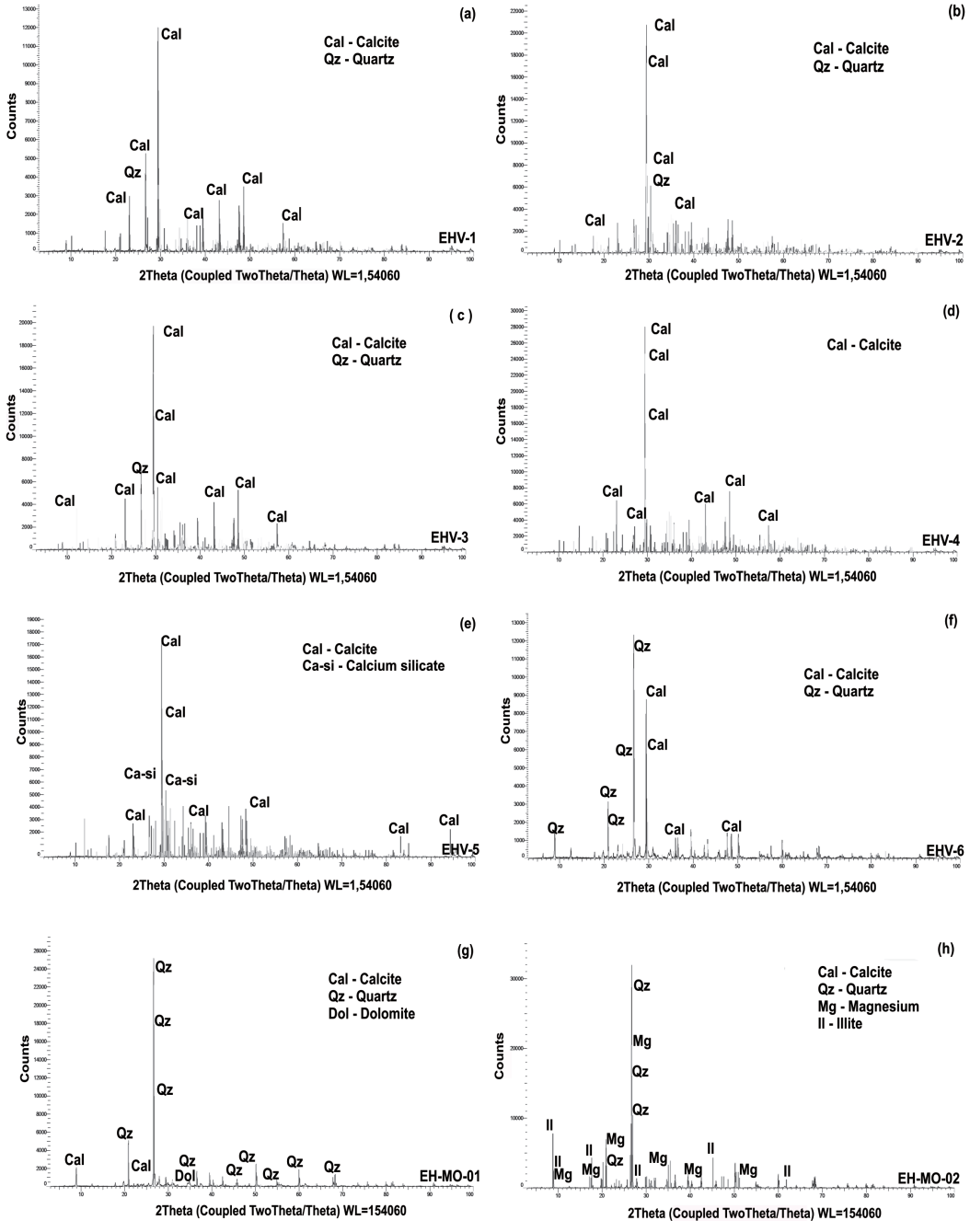

Figure 9. Diffratograms of fine-grained sediments of Elephant Head valley sampling sites.

The group EH_MO_2 and RC_05, and the group EH_06 and EH_MO_1 are explained by their relative spatial proximities. The groups EH_01 and EH_03, and the group EH_02 and EH_04 are explained by their Ca content.

Two principal components explain 97.5% of the total variance. PC1 (93.4%) has high loadings of Si, K, Al, and Fe. The highest scores are associated with Rosmann Cove samples. Negative scores equate to the negative loadings (-0.54) of Ca, associated with Elephant Head Valley (Fig.12b). PC2 (4.3%) has the highest loadings of Ca. The PC1 allows the separation of Elephant Head Valley, the down valley and the blue ice area, and Rossman Cove. In PC1 negative loadings, the PC2 separates the samples with the highest content of Ca (EH-04, EH-05, EH-02) from the lowest content (EH-03, EH-01). In PC1 positive loadings, the PC2 separates the EH-MO-01 sampling site located near the valley

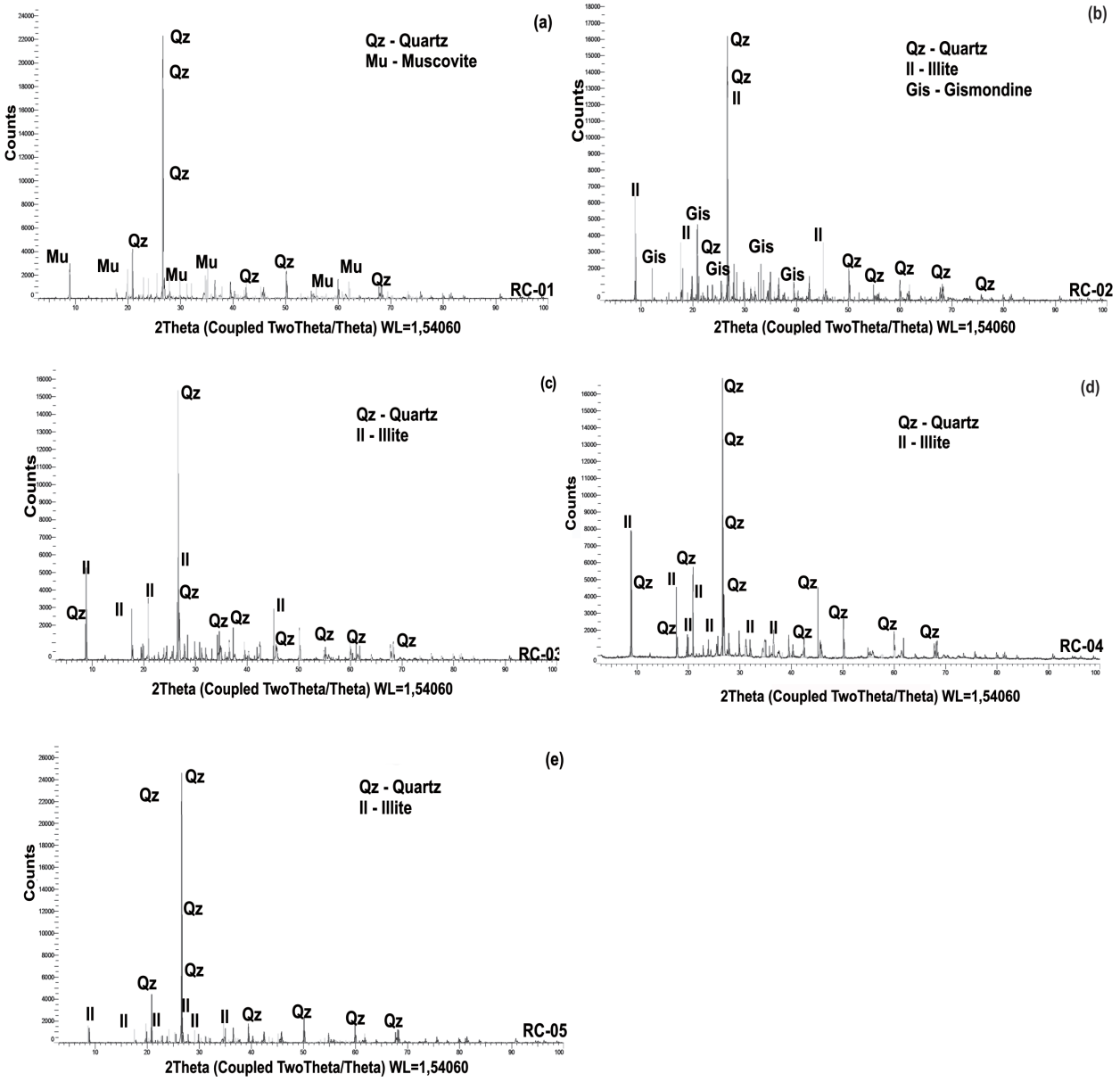

Figure 10. Diffratograms of fine-grained sediments of Rossman Cove sampling sites.

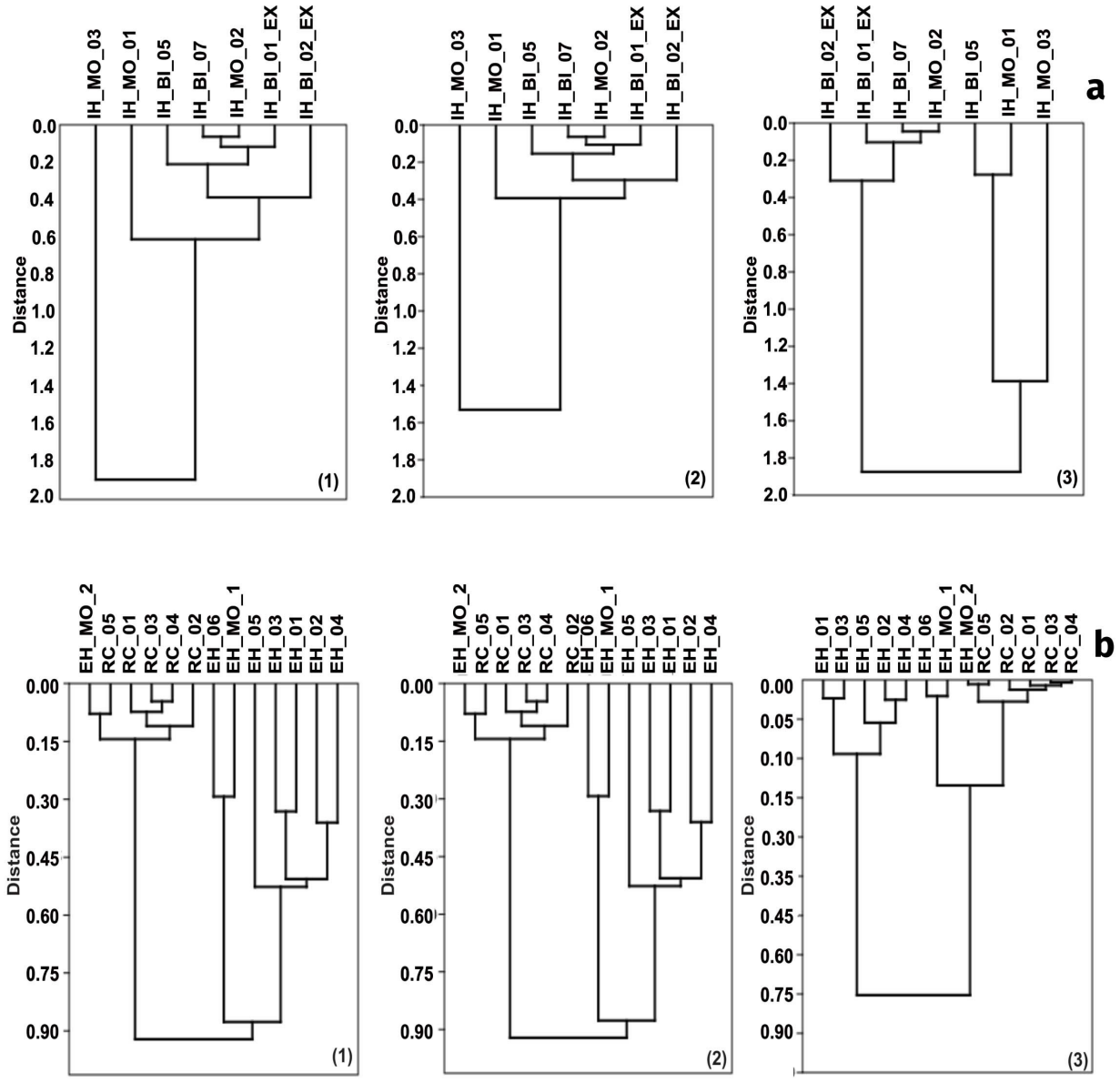

Figure 11. Dendrogram elaborated by Paired (1), Simple (2), and Ward (3) methods in Independence Hills (a), and Union Glacier area (b).

DISCUSSION

Grain size and shape

The fine particles are mainly found in some of the subsurface-derived debris bands which emerge along the blue-ice area margins, as observed in Independence Hills blue-ice moraines (Fig. 2b). As the blue-ice moraines are active zone (Westoby et al. 2016), once reaching the ice surface the exposed finer material is displaced to other areas by the constant and strong wind, prevailing on the moraine coarse and blocky debris. Although the samples were collected in sub-surface ice in Independence Hills, Patriot Hills, and Union Glacier moraines there was not enough fine-grained amount to analyze in the two latter areas (Figs. 2a and f).

A project goal was to identify datasets from the Patriot and Independence blue-ice moraines

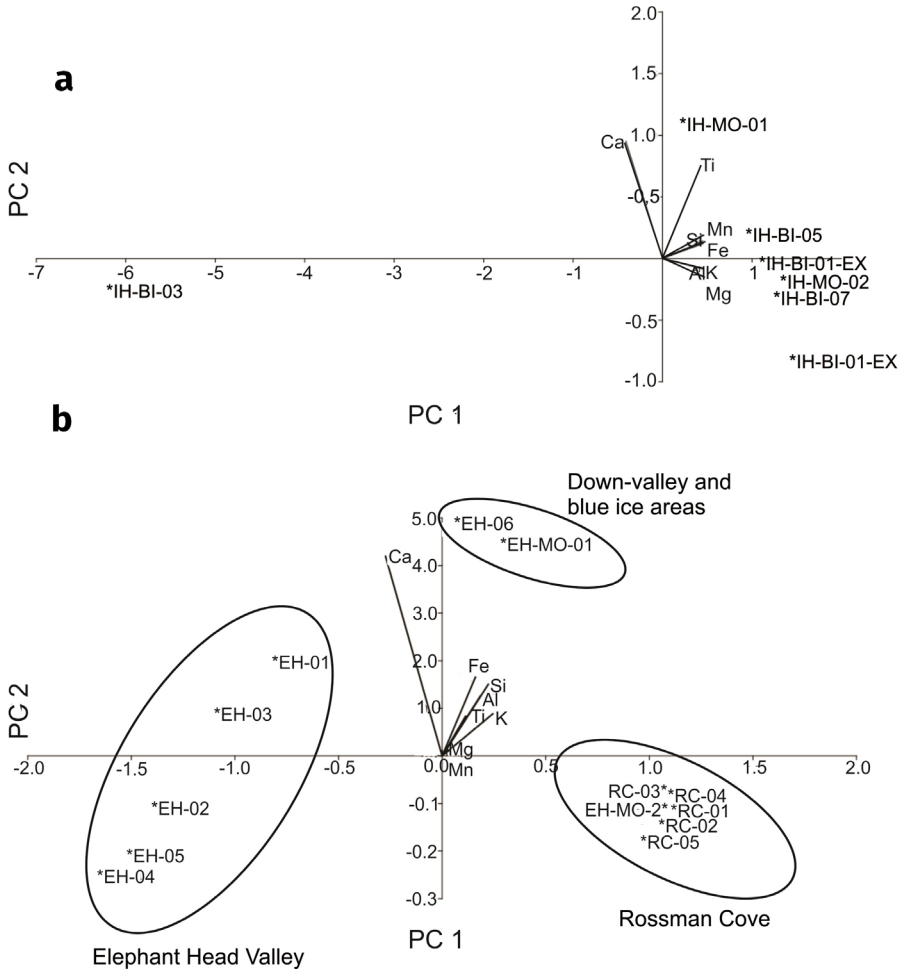

Figure 12. Biplot of the first two components of a Principal Components Analysis for the set of chemical elements in Independence Hills (a) and Union Glacier (b). The circles in Union Glacier area (b) indicate the major areas separated by PC1 vs PC2.

that could indicate subglacially transport and/or wet-based conditions, such as greater roundness of the grains and low C_{40} indexes. Some striated blocks and outcrops were found near the ice surface, indicating possibly such conditions. Winter et al. (2019) proposed that in Horseshoe Valley the basal sediment entrained at the ice/bed interface by repeated melting and refreezing of warm-based ice, and presented the characterization of the surface sediment: (a) subrounded clasts with straight and parallel striations; (b) subangular clasts with multiple striations. In our study, the sediment analyzed in these areas shows a low presence of rounded clasts and the prevalence of subangular and angular ones, high C_{40} values, and the absence of micro-striations (Fig. 4). We follow Winter et al. (2019) about the englacial entrance of clasts along the margins of Horseshoes Valley and their transference toward the blue ice surfaces. Nevertheless, Union Glacier (70km north) is considered a glacier with a frozen bed (Rivera et al. 2010). Bader et al. (2017) presented an alternative proposal to explain the origin of the non-faceted/striated pebbles in Mt. Achernar Moraine, East Antarctica: the debris could originate from and be transported along the bed slowly by cold-based ice. We suggest the entrainment of the sediment not only from glacier bed, but also from both other subaerial and unexposed areas, and passively transported through the ice towards the ice surface, thus submitted to less alteration.

In the Union Glacier area, the high C_{40} values characterize the sediment from Elephant Head, Union Glacier, and Rossman Cove moraines, but they differ from Patriot and Independence Hills by the presence of subangular and subrounded clasts, as shown in Figures 4 and 5.

Sandstone predominates in Patriot Hills and has a major contribution in Independence Hills and Elephant Head morainic material, whereas quartzite predominates in Union Glacier and Rossman Cove moraines (Figs. 6 and 7). All areas show a high proportion of platy clasts (high C_{40} – Fig. 4). As in the area of study, Lukas et al. (2013) observed in several glacial environments in north and south hemispheres that sandstone was related to the clasts with high C_{40}, high RA, and low RWR. Although with the abundant presence of sandstone in Patriot Hills, Independence Hills, and in Elephant Head valley (Fig. 6), subangular clasts dominate in Independence and Patriot Hills, while in Elephant Head valley subrounded clasts prevail (Figure 4). Therefore, specific lithology may not has unique responses to the processes they are exposed (Lukas et al. 2013). Elephant Head is a deglaciated valley with recessional moraines and submitted at present to periglacial conditions, whereas the moraines of Patriot and Independence Hills are composed of englacial debris that emerged at the ice surface.

Distribution of elements and source of the sediment

In general, the chemical composition is differentiated between samples in the Independence Hills suggesting that sediment may have distinct material sources. Debris-band emerging from the blue-ice moraines in parallel ridges indicate that the sediment came from flows caused by internal compressive forces of the glacier. Studies by Rivera et al. (2014b) and Winter et al. (2019) in the blue-ice area of Patriot Hills, using satellite imagery and GPR (Ground-Penetrating Radar) data, identified inner layers that incline more sharply towards the surface. Such layers, according to the study, are associated with the emerged blue-ice moraines composed of materials of heterogeneous geological composition, such as limestone, sandstone, metamorphic and igneous rocks, and other non-volcanic rocks. Figures 8a-g present differentiated mineral concentrations, such as quartz, albite, illite aluminum, and fluorite, suggesting parental rocks and transport at different sites and times, once the morainic ridges ascend to the ice surface at distinct periods (Birtanja 1999, Sinisalo & Moore 2010). The predominant concentration of Ca only in the IH-MO-03 sample, in Independence Hills, may support the distinct material source of the blue-ice morainic ridges.

This distribution of chemical composition displays the contrast between the Elephant Head valley and Rossman Cove sampling sites, reflecting the difference between the sediment sources. Both areas exhibit rocks of the Liberty Hills Formation, which represents variated sediment sources, as thick fluvial and shallow marine to deltaic sequence, composed of basaltic flows, volcanic breccias, conglomerate, quartzite, argillite, and limestone (Webers et al. 1992).

In Elephant Head valley (Figs. 2g and h, and Figs. 9a-f), calcite predominate, followed by quartz, and in Rossman Cove (Figs. 2e, and 10a-e) quartz predominates, followed by illite and muscovite. Illite was identified in soil samples collected in nearby areas and analyzed by Delpupo et al. (2017), associating its origin to the physical fragmentation of micaceous minerals from the parental material. Muscovite is the most common mineral of the mica family and is relatively abundant in sandstone and siltstone (Licht & Hemming 2017). Muscovite is

not especially resistant to chemical weathering. It is quickly transformed into clay minerals. Tiny flakes of muscovite sometimes survive long enough to be incorporated into sediment and immature sedimentary rocks. This means that this sediment and rocks have not been subjected to chemical weathering.

The mineralogical species in the morainic sediment samples in Elephant Head valley correspond to two main peaks: calcite and quartz (Figs. 9a-f). The sand fraction shows a similar parental material composition. Delpupo et al. (2017) found minerals of chlorite, calcite, and halite in the finer fractions of the superficial layers of the soil in this area. The presence of calcite in the clay fraction is evidence of the contribution of the parental material for soil formation. The quartz subpopulation both in the sand and silt-clay fractions may be indicative of the parental rock, namely, sandstone (Basu 1985) and quartzite.

Geological studies have identified sites representing palaeo-shallow marine environments in Heritage Range: carbonate clasts, sandstones, and conglomerates in Edson Hills, Webers Peak, Spring Peak, Bingham Peak, Mount Dolence, and Marble Hills, (Webers et al. 1992, Bugish & Webers 1992), with ages of the formations varying from Middle Cambrian to Permian. In fieldworks grey straight-crested ripples on sandstone, asymmetric ripples within quartzite immediately overlying grey sandstone with flat-crested ripple, and conglomerate boulders with incrusted ripple marks were observed along the Elephant Head valley. The ripples are indicative of water current action rather than wind action and could be interpreted as an ancient shallow sea, as reported by Curtis & Lomas (1999) for the limestone present at other sites of Heritage Range, such as Webers Peaks and Mount Dolence. Vialov (1962) also described this type of mark in Beacon Height West (Victoria Land). Further studies are necessary to confirm or not the existence of this paleoenvironment.

Due to the regional aridity, the polar climate limits chemical weathering and freeze-thaw processes since samples are less exposed to liquid water (Marrero et al. 2018). As reported by Delpupo et al. (2017), and Schaefer et al. (2017), chemical weathering is low in soils and topsoil in the Union Glacier area due to arid conditions. Therefore, it can be inferred that the chemical properties of the sediment were not altered, allowing the preservation and interpretation of provenance of old deposits and sediment (Licht & Hemming 2017). Given the relative lack of liquid water in the interior of Antarctica, comparable with desert environments, the lowest CIA values are recorded where carbonate sediment prevails: Elephant Head valley and IH-MO-03 (Independence Hills). Such preservation is possible because the erosional rates of carbonate are usually lower than that of sandstone in other hyper-arid condition areas of Antarctica (Marrero et al. 2018).

The strong katabatic wind, both in the Patriot and Independence Hills and in the Union Glacier area, acts as an important agent in sediment production and distribution. The snow blown by the wind and its further meltwater spread through the rock walls acting as an important driver in the rare chemical weathering processes, even incipient. Yoshikawa et al. (2000) reported such processes in the Patriot and Independence Hills. Besides, the fine-size material (silt and clay fractions) is removed by the wind, leaving behind medium and coarse sand, pebbles, and boulders. The predominance of sandy fraction in most samples suggests long-term erosion by wind-driven particles and the importance of sediment supply, as reported in Dry Valleys by Marchant & Head (2007).

Sediment provenance

In the region of the Patriot and Independence Hills, calcareous rocks and marbles predominate (Spörli & Craddock 1992, Webers et al. 1992). The lithology, elements concentration, and mineralogical composition observed in Figures 6, 7, and 8 point to sandstone and quartzite as dominant, but the low presence of calcareous rock suggests the exotic lithologies as the source of the sediment that reaches the surface. The same is observed in the Principal Component Analysis (PCA) graph, which aggregates sampling sites of Independence Hills (Fig. 12a-b) with varied chemical elements, individualizing only one sample with the prevalent percentage of Ca – sample IH-MO-03. It is the closest sampling site to the mountain wall, thus interpreting the adjacent mountain slopes as a source of sediment, or far-traveled sediment from the rocks of the interior of Horseshoe Valley, such Liberty Hills and Marble Hills, which correspond to the same type of rock of the Minaret Formation.

Ice sheet model simulation (Winter et al. 2016) suggests that the ice in Horseshoe Valley has not experienced directional change and has remained slow-flowing from the head of Horseshoe Valley toward Patriot Hills and Independence Hills blue-ice areas since the mid-Holocene. It is inferred by Casassa et al. (2004) that the area around Patriot Hills is in a near steady-state, and Horseshoe Valley is thickening, supplied by flow from the inland ice sheet through ice cliffs located in mountains gaps in the Heritage Range. This means that zones of wholly local lithologies occur within the wider spread of lithologies associated with far-traveled material (Sugden & Hall 2020).

Glaciers flow and sediment

It is inferred that the Union Glacier flow pattern is distinct from those operating in the Patriot and Independence Hills area, which is characterized by the ascended material to the ice surface by shear bands within the glacier, formed in areas of compressive ice flow (Hambrey & Glasser 2003, Fogwill et al. 2012, Hein et al. 2016a). Debris brought to the surface ice is accumulated as ablation till, when the adjacent ice sublimates (Figs. 2a-b). Evidence for such shear bands includes the presence of sediment in sub-vertical bands in sections through the ice (Cassidy et al. 1992, Rivera et al. 2014b, Winter et al. 2019).

The moraine observed at the embayment in the Union Glacier margin (Fig. 2d), was initially interpreted by Costa et al. (2017) as supraglacial moraine, and a product of glacier thinning processes and debris input from colluvium on surrounding rock slopes. The thick debris cover cuts off ablation and creates protected moraine-covered ice standing above the bare glacier surface (Fogwill et al. 2012). Earlier studies (Hättestrand & Johansen 2005) used to apply the term “supraglacial” for those moraines that are now labeled as “blue-ice moraines”, although supraglacial moraine differs from the blue-ice moraine with emerging debris to the glacier surface.

Winter et al. (2019) detected by radargrams englacial reflectors which extend from the ice/bed interface to blue-ice moraines in the lee of Independence and Patriot Hills. Kassab et al. (2019) also describe new findings on the Mount Achernar blue-ice moraine, based on GPR data that reveals the internal stratigraphy. However, so far, there is no similar data in the Union Glacier area that could reveal the internal stratigraphy, and confirm the sub-ice and sediment flow in the direction of this moraine.

A similar process could be applied to the moraines in Rossman Cove, which have developed next to the hills (Fig. 2e). However, the sequence of moraine crests and the northeast direction of the tail argue for the influence of the Union Glacier flow on the structure of the deposit, represented by debris accumulation and deformation of the moraine (Fig. 2e). The

medial moraine developed at the narrowest section of the Union Glacier also reflects the glacier flows, but, in this case, it is inferred that the debris accumulated in downslope areas, as at the base of the slopes, is displaced by the tributary glaciers (Figure 2f).

In Independence/Patriot and Union Glacier areas, gravel and sandy gravel predominate at all sampling sites. A high C_{40} index also is present in all sampling sites, which indicates glacial passive transport, but these same values point to distinct processes related to glacier flow and/or slopes/colluvium contribution (Fig. 4). IH-BI-03 sample has clast with the lowest C_{40} value and is individualized in the graph. The sample is also individualized in the histogram of elements concentration (Fig. 7), in the PCA and cluster analysis (Fig. 7, Fig. 11a, and Fig. 12a) by the elevated Ca content. The sample is located near the mountain slopes of carbonate rock that contribute to debris accumulation. Locally derived debris contribution is also suggested in Elephant Head Valley, in Elephant Head Moraine, located at the entrance of the valley in the blue-ice area, and in Rossman Cove (Fig. 7, Fig. 11b and Fig. 12b).

On the other side, the varying Independence (IH) and Patriot Hills (PH) clast shape and geochemical features evidence external contribution by far-traveled englacial transport of debris.

CONCLUSION

This work used granulometric, morphoscopic, and geochemical information from the sediment of morainic deposits of two areas of the Heritage Range, southern sector of Ellsworth Mountains, West Antarctica: Patriot / Independence Hills, and Union Glacier to obtain an interpretation of the control processes on the glacial and sedimentary dynamics. Provenance analysis using geochemical methods on fine-grained sediment in combination with detrital sand and gravel analysis reveals different elements of the glaciological and sedimentary sources and processes.

The geomorphological and sedimentary dynamics of the Union glacier and region of the Patriot and Independence Hills have distinct characteristics, although the regions are approximately 70 km apart and have similar ice mass balance. In both areas, it is possible to infer the primary sediment sources and the post-depositional processes.

Variations in granulometry, shape, chemical and mineralogical compositions in morainic sediment reflect differences between the local sediment transport by the Union glacier flow and the englacial sediment transport in the Patriot and Independence Hills. In Independence/ Patriot and Union Glacier areas, gravel and sandy gravel predominate at all sampling sites. A high C_{40} index is also present in all sampling sites, which indicates glacial passive transport. However, angular and subangular grains dominate in Patriot and Independence Hills sediment, whilst subrounded grains predominate in Rossman Cove, Elephant Head and Union Glacier moraines sediment, followed by subangular clasts, which infers distinct processes acting on the sediments. Low CIA values in all samples reveal very low chemical weathering. In Independence Hills differentiated mineral concentrations, such as quartz, albite, illite, and aluminum, suggest parental rocks and transport at different sites; in the Union Glacier area quartz predominates in Rossman Cove and calcite in Elephant Head valley, inferring local parental rocks. Cluster and PCA allowed the separation of these areas.

Sediment analysis from Patriot and Independence Hills may infer contribution from unexposed basement rocks to the glacial debris bands carried by the ice compression streams, which results in the blue-ice moraines, indicating that fine-grained sediment may represent the comminution of coarser-grained till in distinct spatial and temporal scales.

In contrast, the extensive moraines at the margin of Union Glacier and in Rossman Cove are dominated by locally-derived material and distributed through the area by the flow of the Union Glacier and other tributary glaciers. The geochemical signatures of fine-grained sediment and morphoscopic features of sand and gravel size materials suggest that they were derived mainly from the adjacent rock outcrop. The surface boulders also reflect the local rockfall debris.

The sediment from the morainic deposits makes available information about ice sheet changes and the debris source. Nonetheless, there is a wide and complex range of processes that affect the detrital along the pathway from source to catchment, as revealed by the studies presented in this work.

Thus, further geochemical studies and isotopic analysis, with the collection and processing of ice-penetrating radar data in the area of study, mainly in the Union Glacier area, are necessary to investigate the changing conditions of subglacial topography and ice thickness and flow, which influence the sediment entrainment, transport, and deposition processes, and consequently the formation of moraines.

Acknowledgments

The authors thank the Conselho Nacional de Desenvolvimento Científico e Tecnológico (CNPq) and the Brazilian National Institute for Cryospheric Sciences for financing the research, and the Brazilian Antarctic Program for the expedition logistics. The authors also thank Jorge Arigony Neto (Rio Grande Federal University - FURG) for the ASTER imagery. Special thanks to the reviewers and Kathy Licht for the suggestions and corrections that improved significantly the original manuscript.

REFERENCES

AKÇAR N, YEŞILYURT S, HIPPE K, CHRISTL M, VOCKENHUBER C, YAVUZ V & ŐZSOY B. 2020. Build-up and chronology of blue-ice moraines in Queen Maud Land, Antarctica. Quat Sci Adv 2: 1-13. DOI:10.1016/j.qsa.2020.100012.

ALFONSO JA, VASQUEZ Y, HERNANDEZ AC, MORA A, HANDT H & ELOY SIRA E. 2015. Geochemistry of recent lacustrine sediments from Fildes Peninsula, King George Island, Maritime Antarctica. Antarct Sci 27(5): 462-471. DOI: 10.1017/S0954102015000127.

BADER NA, LICHT KJ, KAPLAN MR, KASSAB C & WINCKLER G. 2017. East Antarctic ice sheet stability recorded in a high-elevation ice-cored moraine. Quat Sci Rev 159: 88-102. DOI: 10.1016 /j .quascirev.2016.12.005.

BASU A. 1985. Reading provenance from detrital quartz. In: ZUFFA GG (Ed), Provenance of Arenites. Dordrecht, Reidel Publishing, 231-247.

BENN DI & BALLANTYNE CK. 1994. Reconstructing the transport history of glaciogenic sediments – a new approach based on the covariance of clast form indices. Sediment Geol 91: 215-227.

BLOTT SJ & PYE K. 2001. Gradistat: A Grain Size Distribution and Statistics Package for the Analysis of Unconsolidated Sediments. Earth Surf Process Landf 26: 1237-1248. DOI: 10.1002/esp.261.

BLOTT SJ & PYE K. 2007. Particle shape: a review and new methods of characterization and classification. Sedimentol 55: 31-63. DOI: 10.1111/j.1365-3091.2007.00892.x.

BIRTANJA R. 1999. On the glaciological, meteorological and climatological significance of Antarctic blue ice areas. Rev Geophys 37(3): 337-359.

BOCKHEIM JG & SCHAEFER CEGR. 2015. Soils of Ellsworth Land, the Ellsworth Mountains. In: BOCKHEIM J (Ed), The Soils of Antarctica. World Soils Book Series. Springer, Cham, p. 169-182. DOI: 10.1007/978-3-319-05497-1_10.

BUGGISH W & WEBERS GF. 1992. Facies of Cambrian carbonate rocks, Ellsworth Mountains, West Antarctica. In: WEBERS GF, CRADDOCK C & SPLETTSTOESSER JF (Eds), Geology and Paleontology of the Ellsworth Mountains, West Antarctica. Geological Society of America, Memoir 170: 81-100. DOI:0.1130/MEM170.

CASASSA G, BRECHER HH, CÁRDENAS C & RIVERA A. 1998. Mass balance of the Antarctic ice sheet at Patriot Hills. Ann Glaciol 27: 130-134. DOI: https://doi.org/10.3189/1998AoG27-1-130-134.

CASASSA G, RIVERA A, ACUÑA C, BRECHER H & LANGE H. 2004. Elevation change and ice flow at Horseshoe Valley, Patriot Hills, West Antarctica. Ann Glaciol 39: 2-28. DOI: 10.3189/172756404781814564l.

CASASSA G, RIVERA A, LANGE H & CÁRDENAS C. 2000. Estudios glaciológicos en Patriot Hills. In: IX Congreso Geológico Chileno, Sociedad Geológica de Chile. Puerto Varas 2: 359-368.

CASSIDY W, HARVEY R, SCHUTT J, DESLISLE G & YANAI K. 1992. The meteorite collection sites of Antarctica. Meteoritics 27: 490-525. DOI:10.1111/j.1945-5100.1992.tb01073.x.

CHEN JL, WILSON CR, BLANKENSHIP DD & TAPLEY BD. 2006. Antarctic mass rates from GRACE. The Cryosph 33(11): L11502. DOI:10.1029/2006GL026369.

CHIPERA SJ & BISH DL. 2013. Fitting full X-Ray diffraction patterns for quantitative analysis: a method for readily quantifying crystalline and disordered phases. AMPC 3: 47-53. DOI: 10.4236/ampc.2013.31A007.

CORTI G, ZEOLI A, BELMAGGIO P & FOLCO L. 2008. Physical modeling of the influence of bedrock topography and ablation on ice flow and meteorite concentration in Antarctica. J Geophys Res 113: 1-18. DOI:10.1029/2006JF000708.

COSTA VCS, VIEIRA R & SIMÕES JC. 2017. Geomorphology and sedimentology of Union Glacier area, Ellsworth Mountains, Occidental Antarctica. Rev Bras Geomorfol 8(3): 579-595. DOI:10.20502/www.ugb.org.br rbg.v18i3.1246.

CRADDOCK C. 1969. Geologic Map of Antarctica, Sheet 4, Ellsworth Mountains. American Geographical Society.

CURTIS ML & LOMAS SA. 1999. Late Cambrian stratigraphy of the Heritage Range, Ellsworth Mountains: implications for basin evolution. Antarct Sci 11(1): 63-77.

DENTON GH, BOCKHEIM JG, RUTFORD RH & ANDERSEN BG. 1992. Glacial history of the Ellsworth Mountains, West Antarctica. In: WEBERS GF, CRADDOCK C & SPLETTSTOESSER JF (Eds), Geology and Paleontology of the Ellsworth Mountains, West Antarctica. Geological Society of America: Colorado, p. 403-432.

DELPUPO CS, SCHAEFER CEGR, ROQUEC MB, FARIA ALL, ROSA KK, THOMAZINI A & PAULA MD. 2017. Soil and landform interplay in the dry valley of Edson Hills, Ellsworth Mountains, Continental Antarctica. Geomorphology 295: 134-146. DOI:10.1016/j.geomorph.2017.07.002.

EVANS DJA & BENN DI (Eds). 2004. A Practical Guide to the Study of Glacial Sediments. London: Edward Arnold, 266 p.

FOGWILL CJ, HEIN AS, BENTLEY MJ & SUGDEN DE. 2012. Do blue-ice moraines in the Heritage Range show the West Antarctic ice sheet survived the last interglacial? Palaeogeogr Palaeoclimatol Palaeoecol 335-336: 61-70. DOI:10.1016/j.palaeo.2011.01.027.

GOMEZ R, ARIGONY-NETO J, DE SANTIS A, VIJAY S, JAÑA R & RIVERA A. 2019. Ice dynamics of Union Glacier from SAR offset tracking. Glob Planet Change 174: 1-15. DOI: 10.1016/j.gloplacha.2018.12.012.

GRALY JA, LICHT KJ, KASSAB CM, BIRD BW & KAPLAN MR. 2018. Warm-based basal sediment and far-field Pleistocene origin evidenced in central Transantarctic blue ice through stable isotopes and internal structures. J Glaciol 64(244): 185-196. DOI: 10.1017/jog.2018.4.

HAMBREY MJ & GLASSER NF. 2003. The role of folding and foliation development in the genesis of medial moraines: examples from Svalbard glaciers. J Geol 111: 471-485. DOI:10.1086/375281.

HÄTTESTRAND C & JOHANSEN N. 2005. Supraglacial moraines in Scharffenbergbotnen, Heimfrontfjella, Dronning Maud Land, Antarctica – significance for reconsgtructing former blue ice areas. Antarct Sci 17(2): 225-236. DOI: 10.1017/S0954102005002634.

HEIN AS, MARRERO SM, WOODWARD J, DUNNING SA, WINTER K, WESTOBY MJ, FREEMAN SPHT, SHANKS RP & SUGDEN DE. 2016a. Mid-Holocene pulse of thinning in the Weddell Sea sector of the West Antarctic ice sheet. Nat Commun 7(12511): 1-8. DOI:10.1038/ncomms12511.

HEIN AS, WOODWARD J, MARREMO SM, DUNNING SA, STEIG EJ, FREEMAN SPHT, STUART FM, WINTER K, WESTOBY MJ & SUGDEN DE. 2016b. Evidence for the stability of the West Antarctic Ice Sheet divide for 1.4 million years. Nat Commun 7(10325): 1-8. DOI:10.1038/ncomms10325.

HOFFMANN K ET AL. 2020. Stable water isotopes and accumulation rates in the Union Glacier region, Ellsworth Mountains, West Antarctica, over the last 35 years. The Cryosph 14: 881-904. DOI: 10.5194/tc-14-881-2020.

HUBBARD B & GLASSER N. 2005. Field Techniques in Glaciology and Glacial Geomorphology. Wiley, Chicherter UK, 400 p.

JOUGHIN I, SMITH BE & MEDLEY B. 2014. Marine Ice Sheet collapse potentially under way for the Thwaites Glacier Basin, West Antarctica. Sci, p. 1-3. DOI:10.1126/science.1249055.

KASSAB CM, LICHT KJ, PETERSSON R, LINDBÄCK K, GRALY JA & KAPLAN MR. 2019. Formation and evolution of an extensive blue-ice moraine in central Transantarctic Mountains, Antarctica. J Glaciol 66(255): 49-60. DOI: 10.1017/jog.2019.83.

KLEIN C & DUTROW B. 2012. Manual de Ciência dos Minerais. Porto Alegre: Bookman, 724 p.

LEE J, RAYMOND B, BRACEGIRDLE T, CHADÈS I, FULLER RA, SHAW JD & TERAUDS A. 2017. Climate change drives expansion of Antarctic ice-free habitat. Nature 547: 49-54, DOI:10.1038/nature22996.

LICHT K & HEMMING SR. 2017. Analysis of Antarctic glacigenic sediment provenance through geochemical and petrologic applications. Quat Sci Rev 164: 1-24. DOI:10.1016/j.quascirev.2017.03.009.

LUKAS S ET AL. 2013. Clast shape analysis and clast transport paths in glacial environments: a critical review of methods and the role of lithology. Earth Sci Rev 121: 96-116.

MARCHANT DR & HEAD JW. 2007. Antarctic dry valleys: microclimate zonation, variable geomorphic processes, and implications for assessing climate change on Mars. Icarus 192(1): 187-222. DOI:10.1016/j.icarus.2007.06.018.

MARRERO SM, HEIN AS, NAYLOR M, ATTAL M, SHANKS R, WINTER K, WOODWARD J, DUNNING S, WESTOBY M & SUGDEN D. 2018. Controls on subaerial erosion rates in Antarctica. Earth Planet Sci Lett 501: 56-66. DOI:10.1016/j.epsl.2018.08.018.

MATSUOKA K ET AL. 2021. Quantarctica, an integrated mapping environment for Antarctica, the Southern Ocean, and sub-Antarctica islands. Environ Model Softw 140 105015, 14 p. DOI: 10.1016/j.envsoft.2021.105015.

MERCER JH. 1978. West Antarctic ice sheet and CO_2 greenhouse effect: a threat of disaster. Nature 271: 321-325.

MILLIKEN KL. 2005. Late diagenesis and mass transfer in sandstone-shale sequences. In: MACKENZIE FT (Ed), Sediments, Diagenesis, and Sedimentary Rocks. Treatise on Geochemistry. London: Elsevier, 190 p.

NAUGHTEN KA, DE RYDT J, ROSIER SHR, JENKINS A, HOLLAND PR & RIDLEY JK. 2021. Two-timescale response of a large Antarctic ice shelf to climate change. Nat Commun 12: 1991. DOI:10.1038/s41467-021-22259-0.

NESBITT HW & YOUNG GM. 1982. Early Proterozoic climates and plate motions inferred from major element chemistry of lutites. Nature 299: 715-717. DOI: 10.1038/299715a0.

PATTYN F & MORLIGHEM M. 2020. The uncertain future of the Antarctic Ice Sheet. Science 367(6484): 1331-1335. DOI: 10.1126/science.aaz5487.

PERKINS D. 2014. Mineralogy. 3° ed. Edinburg: Person, 568 p.

RIGNOT E, MOUGINOT J, MORLIGHEM M, SEROUSSI H & SCHEUCHL B. 2014. Widespread, rapid grounding line retreat of Pine Island, Thwaites, Smith, and Kohler glaciers, West Antarctica, from 1992 to 2011. Geophys Res Lett 41: 3502-3509. DOI:10.1002/2014GL060140.

RIGNOT E, MOUGINOT J & SCHEUCHL B. 2017. InSAR-based Antarctica ice velocity map, version 2. Boulder, Colorado USA, NASA, National Snow and Ice Data Center Distributed Active Archive Center. DOI: 10.5067/D7GK8F5J8M8R.

RIVERA A, CAWKWELL F, WENDT A & ZAMORA R. 2014a. Mapping Blue-Ice Areas and Crevasses in West Antarctica Using ASTER Images, GPS, and Radar Measurements. In: KARGEL J, LEONARD G, BISHOP M, KÄÄB A & RAUP B (Eds), Global Land Ice Measurements from Space. Berlin: Springer. DOI: 10.1007/978-3-540-79818-7_31.

RIVERA A, ZAMORA R, RADA C, WALTON J & PROCTOR S. 2010. Glaciological investigations on Union Glacier, Ellsworth Mountains, West Antarctica. J Glaciol 51(55): 91-96.

RIVERA A, ZAMORA R, URIBE JA, JAÑA R & OBERREUTER J. 2014b. Recent ice dynamic and surface mass balance of Union Glacier in the West Antarctic Ice Sheet. The Cryosphere 8: 1445-1456. DOI:10.5194/tc-8-1445.

SCHAEFER CEGR, MICHEL RFM, DELPUPO C, SENRA EO, BREMER UF & BOCKHEIM JG. 2017. Active layer thermal monitoring of a Dry Valley of the Ellsworth Mountains, Continental Antarctica. Catena 149(2): 603-615. DOI:10.1016/j.catena.2016.07.020.

SINISALO A & MOORE JC. 2010. Antarctic blue ice areas – towards extracting paleoclimate information. Antarct Sci 22: 99-115. DOI:10.1017/S0954102009990691.

SPÖRLI KB. 1992. Stratigraphy of the Crashsite Group, Ellsworth Mountains, West Antarctica. In WEBERS GF, CRADDOCK C & SPLETTSTOESSER JF (Eds), Geology and Paleontology of the Ellsworth Mountains, West Antarctica. Geological Society of America, Memoir 170: 21-35. DOI:10.1130/MEM170.

SPÖRLI KB & CRADDOCK C. 1992. Stratigraphy and structure of the Marble, Independence and Patriot Hills, Heritange Range, Ellsworth Mountains, West Antarctica. In WEBERS GF, CRADDOCK C & SPLETTSTOESSER JF (Eds), Geology and Paleontology of the Ellsworth Mountains, West Antarctica. Geological Society of America, Memoir 170: 365-374. DOI:10.1130/MEM170.

SPÖRLI KB, CRADDOCK C, RUTFORD RH & CRADDOCK JP. 1992. Breccia bodies in deformed Cambrian limestones, Heritage Range, Ellsworth Mountains, West Antarctica. In WEBERS GF, CRADDOCK C & SPLETTSTOESSER JF (Eds), Geology and paleontology of the Ellsworth Mountains, West Antarctica. Geological Society of America Memoir 170: 365-374.

SUGDEN DE & HALL A. 2020. Antarctic blue-ice moraines: analogue for Northern Hemisphere ice sheets? Quat Sci Rev 249: 106620. DOI:10.1016/j.quascirev.2020.106620.

SUGDEN DE, HEIN AS, WOODWARD J, MARRERO SM, RODÉS A, DUNNING SA, STUART FM, FREEMAN SPHT, WINTER K & WESTOBY MJ. 2017. The million-year evolution of the glacial trimline in the southernmost Ellsworth Mountains, Antarctica. Earth Planet Sci Lett 469: 42-52. DOI: 10.1016/j.epsl.2017.04.006.

TURNER J ET AL. 2019. The dominant role of extreme precipitation events in Antarctic snowfall variability. Geophys Res Lett 46: 3502-3511. DOI: 10.1029/2018GL081517.

TURNEY CSM, FOGWILL CJ, VAN OMMEN TD, MOY AD, ETHERIDGE D, RUBINO M, MARK AJ, CURRAN MAJ & RIVERA A. 2013. Late Pleistocene and early Holocene change in the Weddell Sea: a new climate record from the Patriot Hills, Ellsworth Mountains, West Antarctica. J Quat Sci 28(7): 697-704. DOI: 10.1002/jqs.2668.

TURNEY CSM ET AL. 2019. Early last Interglacial ocean warming drove substantial ice mass loss from Antarctica. PNAS 117(8): 3996-4006. DOI: 10.1073/pnas.1902469117.

VIALOV OS. 1962. Problematica of the Beacon Sandstone at Beacon Height West, Antarctica. New Zeal J Geol Geop 5: 718-732.

VIEIRA R, HINATA H, ROSA KK, ZILBERSTEIN S & SIMÕES JC. 2012. Periglacial features in Patriot Hills, Ellsworth Mountains, Antarctica. Geomorphology 155-156: 96-101. DOI:10.1016/j.geomorph.2012.12.014.

VIEIRA R & SIMÕES JC. 2011. Geomorfologia Glacial dos Montes Patriot e Independence, Montanhas Ellsworth, Manto de gelo da Antártica Ocidental. Rev Bras Geomorfol 12: 45-58.

WEBERS GF, BAUER RL, ANDERSON JM, BUGGISCH W, OJAKAS RW & SPÖRLI KB. 1992. The Heritage Group of the Ellsworth Mountains, West Antarctica. In WEBERS GF, CRADDOCK C & SPLETTSTOESSER JF (Eds), Geology and Paleontology of the Ellsworth Mountains, West Antarctica. Geological Society of America, Memoir 170: 9-19. DOI:10.1130/MEM170.

WENDT A ET AL. 2009. Reassessment of ice mass balance at Horseshoe Valley, Antarctica. Antarct Sci 21: 505-513.

WESTOBY MJ, STUART A, DUNNING SA, WOODWARD J, HEIN AS, SHASTA M, MARRERO SM, WINTER K & SUGDEN DE. 2016. Interannual surface evolution of an Antarctic blue-ice moraine using multi-temporal DEMs. Earth Surf Dynam 4: 515-529. DOI:10.5194/esurf-4-515-2016.

WINTER K ET AL. 2016. Assessing the continuity of the blue ice climate record at Patriot Hills, Horseshoe Valley, West Antarctica. Geophys Res Lett 43: 2019-2026. DOI:10.1002/2015GL066476.

WINTER K ET AL. 2019. Radar-detected englacial debris in the West Antarctic Ice Sheet. Geophys Res Lett 46(10): 454-462. DOI:10.1029/2019GL084012.

WINTHER JG, JESPERSEN MN & LISTON GE. 2001. Blue ice areas in Antarctica derived from NOAA AVHRR satellite data. J Glaciol 47: 325-334.

YOSHIKAWA K, ISHIMARU S & HARADA K. 2000. Weathering of Paleozoic marbles in the Independence Hills and Patriot Hills, Ellsworth Mountains, Antarctica. Phys Geogr 21(6): 568-576. DOI: 10.1080/02723646.2000.10642726.

SUPPLEMENTARY MATERIAL

Figure S1.
Tables SI, SII.

How to cite
COSTA V, ROSA KK, SANDES A, DELPUPO C & VIEIRA R. 2022. Sedimentary evidence of glacial entrainment at Patriot Hills and Union Glacier moraines, Ellsworth Mountains, West Antarctica. An Acad Bras Cienc 94: e20210114. DOI 10.1590/0001-3765202220210114.

Manuscript received on February 3, 2021;
accepted for publication on July 19, 2021

VANESSA COSTA[1]
https://orcid.org/0000-0003-4909-5365

KÁTIA K. ROSA[3]
https://orcid.org/0000-0003-0977-9658

ALLAN SANDES[2]
https://orcid.org/0000-0003-4535-1181

CAROLINE DELPUPO[4]
https://orcid.org/0000-0001-5055-3963

ROSEMARY VIEIRA[1]
https://orcid.org/0000-0003-0312-2890

[1]Universidade Federal Fluminense, Instituto de Geociências, Departamento de Geografia, Av. Gal. Milton Tavares de Souza, s/n, Boa Viagem, 24210-346 Niterói, RJ, Brazil

[2]Universidade Federal Fluminense, Instituto de Geociências, Av. Gal. Milton Tavares de Souza, s/n, Boa Viagem, 24210-346 Niterói, RJ, Brazil

[3]Universidade Federal do Rio Grande do Sul, Centro Polar e Climático, Departamento de Geografia, Av. Bento Gonçalves, 9500, 91501-970 Porto Alegre, RS, Brazil

[4]Instituto Federal de Minas Gerais, campus Ouro Preto, Rua Pandiá Calógeras, 898, Bauxita, Morro do Cruzeiro, 35400-000 Ouro Preto, MG, Brazil

Correspondence to: **Rosemary Vieira**
E-mail: rosemaryvieira@id.uff.br

Author contributions

Costa, V. performed the sample preparation (Union Glacier), sediment analysis, interpretation of the satellite images and results, and writing the manuscript. Vieira, R. contributed to the sediment sampling and analysis, interpretation of the results, and writing the manuscript. Sandes, A. carried out the geochemistry analysis and interpretation of the results. Delpupo, C. contributed to the interpretation of the results of the geochemistry analysis. Rosa, K. contributed to the sample preparation (Patriot and Independence Hills), satellite image interpretation, and interpretation of the results. All authors discussed the results and contributed to the final version of the manuscript.